**FINAL REPORT**

**on**

**US DOT SBIR PHASE 1 PROJECT**
**CONTRACT NUMBER: DTRT5715C10023**

# A Novel Approach to Establishing Remaining Strength of Line Pipe and Fittings with Corrosion Type Defects

**CONTRACT PERIOD OF PERFORMANCE**
**January 29, 2015 – October 28, 2015**

**FINAL REPORT - PERIOD OF PERFORMANCE**
**January 29, 2015 – October 28, 2015**

**by**

**Principal Investigator/Project Manager: Drs. Gery Wilkowski / Prabhat Krishnaswamy**
**Project Team: Drs. Yunior Hioe, Do-Jun Shim, Edward Punch, Mr. Russ Hattery and Mr. Mike Fishman**
**[Subcontractors: Kiefner & Associates, and BN Leis Consulting, Columbus, OH]**

**for**

**US DOT Program Contacts: Mr. James Merritt (Contracting Officer Representative)**
**Ms. Linda Byrne (Contracting Officer)**
**Ms. Melissa Wong (DOT SBIR Program Manager)**

**on**

**October 27, 2015 (Rev.1 – 1/05/2016)**

**ENGINEERING MECHANICS CORPORATION OF COLUMBUS (Emc$^2$)**
**3518 RIVERSIDE DRIVE, SUITE 202**
**COLUMBUS, OHIO 43221-1735**
**Phone: 614-459-3200**
**E-mail: gwilkows@emc-sq.com ; kswamy@emc-sq.com**

# FINAL REPORT

**on**

# A Novel Approach to Establishing Remaining Strength of Line Pipe and Fittings with Corrosion Type Defects

## US DOT SBIR PHASE 1 PROJECT
## CONTRACT NUMBER: DTRT5715C10023

**REPORTING PERIOD: January 29, 2015 – October 28, 2015**

This is the *Final Report* on the above project that started on January 29, 2015 and terminated on October 28, 2015. The total amount obligated under the above contract was $150,000.

As required in the contract this *Final Report* is organized into the following sections:

a. Summary of the work performed during the period of performance,
b. Significant findings, problems, delays, inclusions, events, trends, etc. occurring during the period of performance,
c. Description and schedule of the future work needed for further development of new non-destructive evaluation methods to quantify remaining strength of line-pipe steel and/or line-pipe fittings, and
d. Recommendations to the government that may assist in development of this contract.

Also, as required in the contract the following attachments are provided:

a. Final Project Summary Report (Attachment J.1): This Attachment may be used by the Government to communicate the accomplishments of the DOT SBIR Program, both within and outside the Department, as part of the DOT SBIR Program's Brochure.
b. Phase I Commercialization Report (Attachment J.2): The Commercialization Report may be used by the Government for program measurement purposes within the Department of Transportation and Small Business Administration.

# SUMMARY OF WORK - PROJECT ACCOMPLISHMENTS

As stated in Emc$^2$'s Phase 1 proposal this work was designed to establish the feasibility of extending the current technology and computational methods used to assess the remaining strength of higher grade pipelines and fittings with *natural corrosion type areal defects* with a failure criterion that accounts for the transitional changes from a sharp crack to generally thinned regions.

Emc$^2$ and their subcontractors have successfully demonstrated the following;

- A review of past work at DNV/GL and Battelle/PRCI was conducted to determine the accuracy of the existing models in predicting the failure pressure for corroded pipe. The accuracies of the various models were compared using an extensive database. There is a

much smaller database of higher-grade pipe tests with simulated corrosion. Those tests had constant depth machined flaws to simulate corrosion. The constant depth flaw shape makes the B31G model underpredict the failure pressure. Future corroded pipe tests are suggested, but it was recommended by all groups that smooth flat-bottom constant depth flaws should not be used, i.e., more irregular flaw shapes as found in service are a better test of the effective area concepts used.

- A small finite element sensitivity study was conducted to assess the equivalent flaw depth assumptions in the various B31G type analyses. In all the B31G-type analyses, the maximum corrosion depth is reduced to have a constant depth while keeping the maximum length so there is an equivalent area with the variable flaw shape. The amount of the depth reduction is determined from the flaw shape factor. For B31G the shape-factor is 0.666 (assuming the corrosion is bounded by a parabolic flaw shape), while with Modified B31G a flaw-shape factor is 0.85. From circumferential flaw work on nuclear piping, similar studies show that the maximum depth should be used with an equivalent length, i.e., the flaw shape factor is applied to the length rather than the depth. The FE sensitivity studies for axial flaws conducted in this project showed that the equivalent length is also more accurate for axial flaws. The equivalent length approach predicted a lower failure pressure than the equivalent depth assumption; however, the B31G-type analyses with a flow stress of SMYS+10ksi were conservative in predicting the failure pressure, and perhaps using the ultimate strength with the equivalent depth approach would be better in the future and give more consistency across higher grades of pipe.
- The feasibility of using Precise Assessment of Natural Corrosion via Computation ($PANC^2$) methodology for modeling *actual corrosion defect geometries* was conducted using data made available by one major North American pipeline company from their in-line inspection.
- Existing failure criteria as described in ASME B31G [1] for X70 and higher grades of line-pipe steels may need to be modified based on the selected laboratory experiments conducted during this effort.
- The B31G procedures are not applicable to some conditions of interest, i.e., higher longitudinal stress regions, flaws with significant circumferential dimensions, closely spaced flaws and their interactions, and
- That a 'cloud-based' high-performance computational (HPC) system for rapid-time assessment of corrosion type defects in all grades of line-pipe steels is achievable at the end of the Phase II effort.

Figure 1 shows both the corrosion profile in a 36-inch diameter pipe as received from a sample scan provided for this program by a major North American pipeline company and the three-dimensional finite element mesh developed from this profile using the breakthrough $PANC^2$ methodology from this Phase 1 effort. Once such an accurate simulation of an actual corrosion profile is available, finite element (FE) analysis may be conducted using either a commercial software package such as ABAQUS (used in this effort), or an open source FE program available on the 'cloud' to conduct real time simulation and prediction of the failure behavior for each individual case. More specifically, this approach (i) provides a direct evaluation of combined loading of the pipe under internal pressure and axial loading, (ii) determines the effect of notch acuity as actual corrosion profiles have varying radii at the root of the areal defects from sharp

flaws in pits to very blunt general corroded areas, (iii) can handle circumferential oriented corrosion with pressure and axial loading, and (iv) can identify interactions of adjacent corrosion locations on the failure behavior of the pipe.

The above approach promises to be more accurate and possibly superior to the semi-empirical approaches currently used in ASME B31G [1], in predicting failure pressures and margins of safety for actual defects without resorting to equivalent flaw approaches to simplify the analyses. More importantly, the proposed approach can be integrated with advanced corrosion-measuring technologies to rapidly generate accurate failure predictions that will facilitate in-the-field repair decisions.

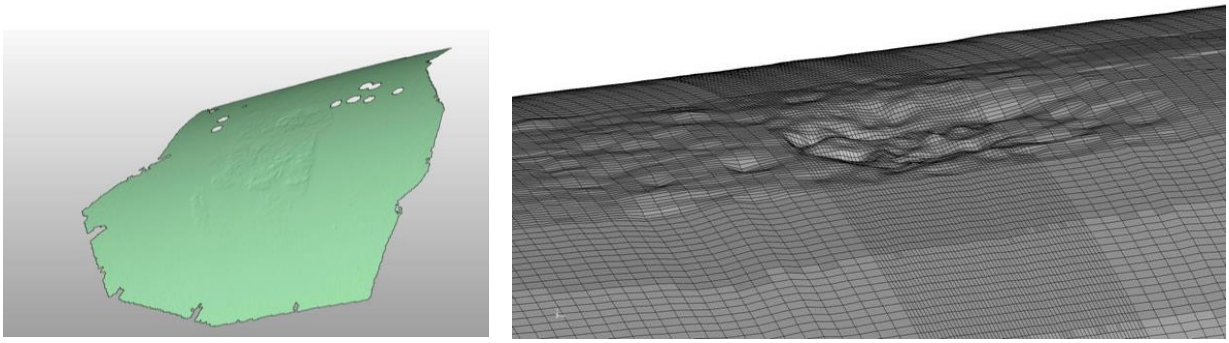

**(a)** **(b)**

**Figure 1 (a) Sample corrosion profile data provided by a North American pipeline company from in-line inspection results, and, (b) three-dimensional finite element mesh (close up) of profile using the PANC$^2$ methodology to simulate natural corrosion to assess remaining strength**

For the above approach to work successfully it is critically important to develop and implement numerically the most appropriate and accurate failure criterion for corrosion type defects based on experimental data. Therefore, the experimental work in this project involved testing single-edge-notched tension (SENT) specimens with varying notch acuity values to failure. These specimens were machined from two different grades of steel, a 1960 vintage X52 which represents the grade used to develop the data that forms the basis of predicting the current remaining strength approaches, and modern X80, a higher grade which is of specific interest in this project, since data have shown the traditional approaches may not be applicable to the higher grade steels. The experimental data from the SENT tests show that the failure behavior is clearly different for the two different grades of steel and that the failure criterion implemented into any analysis method must account for these differences.

Figure 2 shows the Crack-Mouth-Opening Displacement (CMOD) at maximum load in the SENT as a function of notch acuity values used in the SENT specimens for the two grades of steel. As seen from these results, the higher strength X80 steel is much less sensitive to notch acuity and the CMOD values are higher and constant as a function of notch acuity above 0.01 inches. The lower grade X52 material, on the other hand, is much more sensitive to notch acuity as the CMOD values are much lower for the sharper cracks (lower notch acuity values), and increase gradually with higher notch tip radii. Hence the detailed shape at the bottom of the corrosion flaw may be more important for older and newer line pipe.

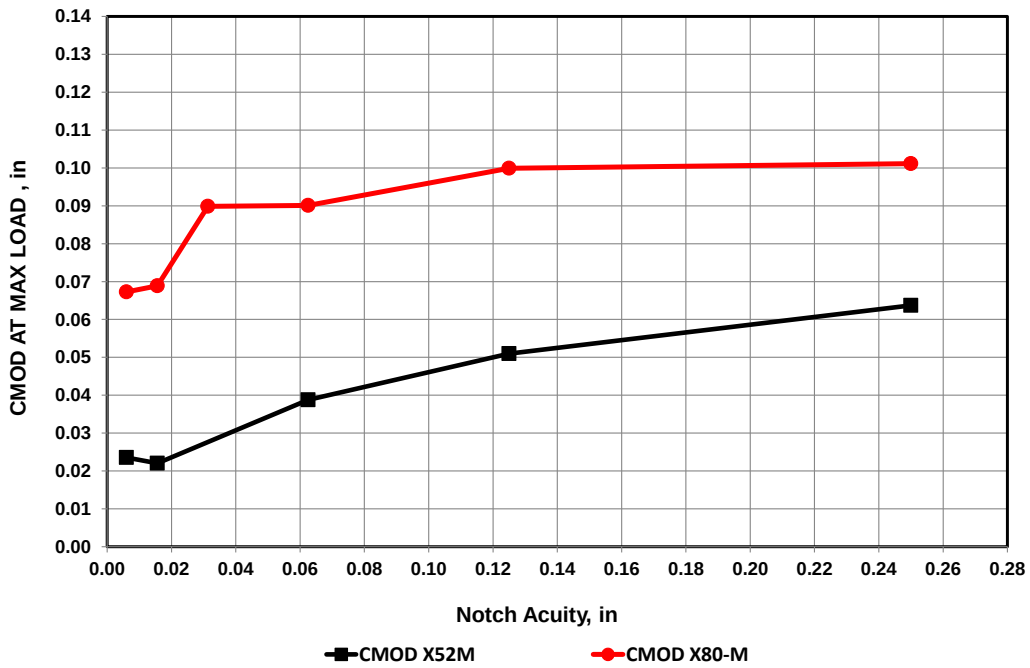


**Figure 2 CMOD at maximum load for transverse SENT specimens machined from vintage X52 and modern X80 grade pipeline steels**

After the successful demonstration of the PANC$^2$ methodology to develop natural corrosion FE meshes and establishing that failure criteria must account for the grade of the material, the balance of the Phase 1 effort focused on sample finite element analyses using actual material property data from vintage low-grade (X52) and modern high-grade (X80) steels using the natural corrosion mesh developed using PANC$^2$ to confirm that there are no numerical instabilities in the computation process and that PANC$^2$ provides reproducible results using the FE mesh from the actual case described above. The sample FE mesh cases from the PANC$^2$ approach ran successfully on both commercial software FE package such as ABAQUS as well as on an open source FE code called WARP3D that Emc$^2$ has modified and is hosted as a 'cloud' based application at the Ohio State University's Ohio Supercomputer Center on a completely independent DOE project on High Performance Computation (HPC). The feasibility of using HPC for rapid-time evaluation of the remaining strength of corroded pipeline and fittings was demonstrated with sample runs. Typically HPC runs on a supercomputer cluster are far more efficient than those on 8-processor servers by at least a factor of 50, and this was confirmed for these cases during this effort.

Accomplishment of these three major objectives summarized above provides a basis for moving forward with the Phase 2 SBIR project.

# SIGNIFICANT FINDINGS BY PROJECT TASKS

The various tasks conducted during this project were as follows:

Task 1 – Review of B31G for X70 and Higher Grade Pipe & Fittings
Task 2 – Experiments for Preliminary Failure Criteria for Blunt Flaws
Task 3 – Leak versus Break Predictions
Task 4 – Precise Assessment of Natural Corrosion via Computation ($PANC^2$) Methodology
Task 5 – Confirm Feasibility of $PANC^2$, and
Task 6 – Program Management, Coordination, and Deliverables

A description of the work performed and significant findings on each of these tasks is detailed in the following sections to substantiate the conclusions above.

## *TASK 1 – REVIEW OF B31G FOR X70 AND HIGHER GRADE PIPE & FITTINGS*

***Review by Dr. John Kiefner***

Under a subcontract to $Emc^2$, Dr. John Kiefner, of Kiefner and Associates (www.kiefner.com) led the work on this task which was reviewed and assessed by $Emc^2$ staff. Dr. Kiefner is an internationally recognized authority in this technical area and developed the original acceptance criteria based on extensive experimental pipe burst tests with corrosion type defects in oil and gas pipelines since the 1960s. He was involved in the development of both the Original and Modified B31G criteria and RSTRENG methodology for predicting the failure behavior of corroded pipelines and fittings. He completed the review of recent relevant literature in this technical area including the Advantica/GL reports for DOT/PRCI and the Battelle/PRCI Report on Project EC 2-5 titled "*Assessing Corrosion Severity for High-Strength Steels,*" dated March 13, 2013 under Contract No. PR-003-103603. Mr. Hans Deeb of PRCI provided a copy of this report to $Emc^2$ and Kiefner & Associates for review and use in this project. Appendix A provides a copy of this review report and is included for completeness.

In Dr. Kiefner's review report he initially summarizes the Original B31G, Modified B31G, RSTRENG, and other Models (i.e., PCORR, LPC-1, and SHELL92). The review was quite extensive for the "Advantica/GL studies" work partially funded by DOT, and more recent PRCI funded efforts that have been completed (EC2-5 was completed and reviewed, but EC2-7 is ongoing and has not been reviewed).

Some important comments from the Kiefner review of these documents relative to this project are given below, *(with some additional $Emc^2$ comments in parenthesis and italicized*).

**Review of Advantica/GL Projects**

1. In the Advantica study, 133 tests with actual corrosion and180 tests with machined flaws in X70 and lower grade steel pipes were used to examine various metal-loss assessment methods. Most of the machined flaw cases had constant depths of corrosion over the length of the corrosion. The Original B31G and Modified B31G assume the flaw depth varies, so these analyses are more likely to over-predict the failure pressure when the

flaw depths are constant. The RSTRENG method had the least variability in the failure pressure predictions for actually corroded pipe since it better accounts for the depth variation with length. Moreover, it works for uniform-depth defects as well.

| Model | $P_{actual}/P_{predicted;}$ Distribution | |
|---|---|---|
| | Mean | Standard Deviation |
| ASME B31G | 1.330 | 0.468 |
| Modified ASME B31G | 1.184 | 0.285 |
| RSTRENG | 1.170 | 0.177 |
| LPC-1 | 1.178 | 0.318 |
| PCORRC | 1.191 | 0.310 |
| SHELL92 | 1.436 | 0.407 |

2. The Advantica study suggests that further evaluations of the models should be made by conducting burst tests on higher-grade materials (i.e., X80 and X100) using defects that are designed to simulate actual corrosion-caused metal loss rather than uniform-depth machined defects.
3. The GL Phase 1 work (DOT/PRCI funded) involved the assessment of corrosion in higher strength pipe. In this work FE analyses were also used for predicting failure with strain-hardening of the material until the von Mises equivalent stress reached the ultimate tensile strength as the failure criterion. There were 8 burst tests and 37 ring-expansion tests of two X80 materials with uniform-depth machined flaws.
4. The Y/T ratios of the X80 materials were low enough that they do not represent low strain-hardening material behavior (a Y/T of 0.93 is now the API 5L limit for all grades of line pipe). The summary tables for the X80 and X100 pipe tests are shown as Table 2 and Table 3 respectively below. The X100 pipe had a Y/T of 0.98 which raises the question of the appropriateness of the flow stress definitions traditionally used (i.e., 1.1*SMYS or SMYS+10,000 psi).

**Table 2 Ranges of ratios of actual to predicted failure pressures from tests done as part of the GL Phase 1 work – 8 burst tests of X80 pipe**

| | **B31G** | **MOD B31G** | **RSTRENG** | **LPC-1** |
|---|---|---|---|---|
| **MAX** | 1.443* | 1.195 | 1.232 | 1.176 |
| **MIN** | 0.67** | 0.745** | 1.099 | 0.993 |
| **RANGE** | 0.773 | 0.45 | 0.133 | 0.183 |
| **AVG** | 1.161 | 1.057 | 1.180 | 1.116 |

*B31G defaulted to the remaining thickness and infinite length for the $4.5\sqrt{Dt}$ cases.
**These low values result because these models consider metal loss areas that are less than the actual areas.

**Table 3 Ranges of ratios of actual to predicted failure pressures from tests done as part of the GL Phase 1 work – 4 burst tests of X100 pipe**

| | **B31G** | **MOD B31G** | **RSTRENG** | **LPC-1** | **Finite Element** |
|---|---|---|---|---|---|
| **MAX** | 1.175* | 1.021 | 1.136 | 1.045 | 1.299 |
| **MIN** | 0.909** | 0.897** | 1.012 | 0.96 | 1.027 |
| **RANGE** | 0.266 | 0.124 | 0.124 | 0.085 | 0.272 |
| **AVG** | 1.04 | 0.959 | 1.074 | 1.001 | 1.115 |

* B31G defaulted to the remaining thickness and infinite length for the cases where the lengths exceeded $4\sqrt{Dt}$.
** These low values result because these models consider metal loss areas that are less than the actual areas.

5. The lower Actual/Predicted values for the B31G and Modified B31G are the result of the flaws being of uniform depth, while the analysis assumes the area of the flaw is either 67% (B31G) or 85% (Modified B31G) of the rectangle that encloses the flaw.
6. The lowest number was associated with a test involving a notch-like groove that may not have represented corrosion-caused metal loss very well. The authors of the GL Phase 1 work also suggest conducting tests on higher-strength materials with defects created by corrosion-like metal removal methods that would result in defects that look more like actual corrosion defects.
7. The GL Phase 2 work was conducted to evaluate the effects of bi-axial stress, cyclic pressure loading, low toughness, and the interaction of closely spaced defects on the ability to accurately predict failure pressures of corroded pipe using the B31G/RSTRENG suite of assessment methods. This work is detailed in separate reports.
8. Tensile test results showed that the Y/T values can differ significantly in the longitudinal and hoop directions (transverse Y/T values were 0.90 to 0.93, while longitudinal Y/T values were 0.77 to 0.87). (*Hence axial stress components may be more important when the Y/T ratios are lower in the longitudinal direction.*[*]*)*
9. Two additional X100 burst tests were conducted using a spherical-shaped machining tool. The experimental/predicted values are shown in Table 4 below.

**Table 4 Actual/Predicted failure pressure of burst tests from GL work on X100 pipe with flaws using a spherical shaped cutter**

| Test# | Orig B31G | | Mod B31G | | RSTRENG/KAPA | | LPC-1 | Shell92 |
|---|---|---|---|---|---|---|---|---|
| | GL | KAI | GL | KAI | GL | KAI | GL | GL |
| **1** | 1.08 | 1.02 | 0.88 | 0.84 | 0.97 | 0.96 | 1.00 | 1.03 |
| **2** | 1.15* | 0.80* | 0.88 | 0.88 | 0.97 | 0.99 | 0.94 | 1.01 |

*These values differ significantly because GL used the 2/3 factor whereas KAI assumed the defect to be of uniform depth and infinite length. The length of the defect was exactly at the upper limit for the use of the 2/3 factor and B31G suggests a default to the maximum depth and infinite length (i.e., the Barlow formula) at that length ($L=4.5\sqrt{Dt}$).

**Review of Battelle/PRCI Report EC 2-5**

1. The authors of EC 2-5 delineated high-strength pipe as being X70 and greater, while all other pipes were considered vintage pipes. *(Actually new X65 and lower grade pipes are considerably different than older X65 and lower grade pipes. The microstructure and inclusion contents differ, so some care is needed in understanding old versus new lower grade steels yet.)*
2. The Report EC 2-5 (Battelle) authors also analyzed the GL database, although they note that GL did not include some critical parameters to properly analyze the database (i.e., only D/t ratios and $L/\sqrt{Dt}$ ratios not actual diameters, wall thicknesses, and flaw lengths were given). Battelle subsequently was able to access these parameters by signing a non-disclosure agreement. Battelle added four additional burst tests (Fluxys data on modern X70 pipe), and a database of unflawed pipe burst tests on high-strength steel pipes.
3. The Fluxys burst tests were on two X70 steels, and four tests were conducted with multiple flaws in each pipe test. In a particular pipe test, the length and depths were the

[*] *Additional Emc$^2$ comments in parenthesis and italicized.*

same, but the width was changed; and the widest flaw was the one that failed. *(This perhaps is related to the fact that with a wider corrosion area the pipe has a higher R/t so more bulging occurring with that wider flaw).* The Battelle authors indicate that this means that flaw width should be included as a parameter in any future failure model for corroded pipe.

4. The Battelle authors suggest there is little value to the ring expansion tests since the wall loss is constant across the width and there is no bulging, hence ring expansion tests do not providing information on shape factors that could be used for actual corrosion.
5. In Task III of the EC 2-5 report, the authors note that corrosion flaws could be susceptible to pressure reversals, which was also observed in some earlier NG-18 work on vintage pipe. (*Generally this occurs closer to the failure pressure, where there could be some flaw growth by primary creep. None of the test data we looked at showed any monitoring of the start of tearing within the corrosion flaw (an aspect evaluated in the SENT tests shown later from this program). Natural corrosion flaws may have some localized slightly deeper areas (see Figure 1) where the start of tearing would be more focused, while that may not occur with machined flaws of constant depth.)*
6. The Battelle team created artificial corrosion flaws by making a dam around the area to be corroded, and using a salt solution and applying an electric current with a copper pad over the area. *(The result was actual corrosion, but still the flaw bottom was smoother than if the corrosion had occurred in the field. Hence these artificial corrosion flaws were not too much different than a smooth machined flaw of relatively constant depth. In some flaws they made a second "nested" corrosion flaw, which was again relatively smooth constant thickness patch.)*
7. In the EC 2-5 report the Battelle team compared 19 pipe burst tests with machined/simulated corrosion on X70 and higher steels to RSTRENG and PCORRC. Although RSTRENG could handle the "nested" flaw cases, the predictions for those flaws were more conservative than other machined/simulated flaw tests as shown in Figure 3 below. The PCORRC model predictions were found to be more accurate for the cases it could handle, but it could not handle the "nested" flaw cases.

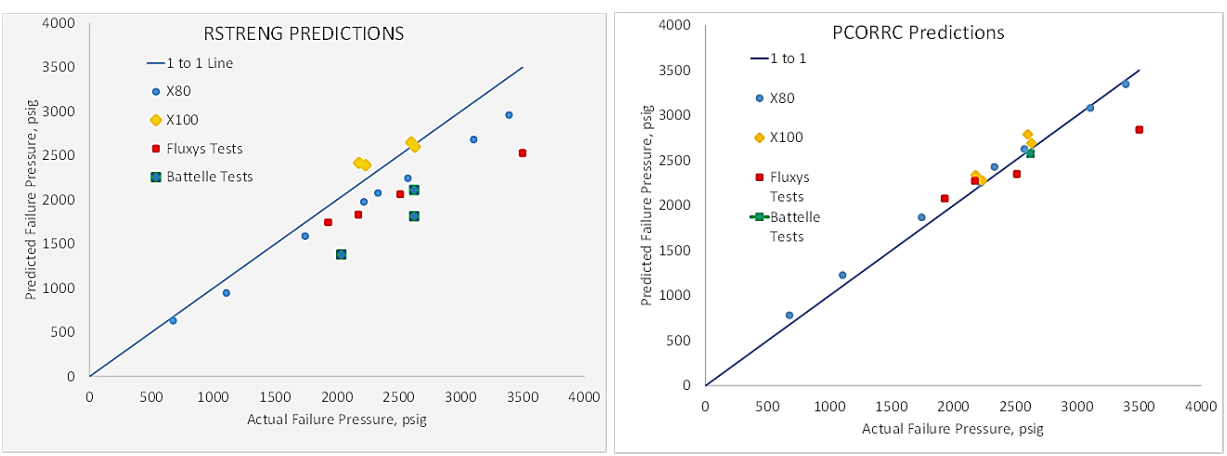


**Figure 3 Comparisons for X70 and higher grade pipe cases with machined/simulated tests from EC 2-5**

8. In EC 2-5, the authors assert that the through-wall failure stress prediction model (axial through-wall-flaw limit-load equation) is useable to determine whether the failure of a given corrosion anomaly will be a leak or a rupture. They noted (correctly) that the B31G models do not predict whether the failure will occur as a leak or as a rupture.
9. In Task 5 of EC 2-5, finite element analyses were conducted to assist in determining if there could be a smooth transition in the failure prediction from lower grade steels to higher grade steels using a different definition of flow stress (or reference stress). Different yield surface criteria were examined, i.e., von Mises, Tresca, and the Battelle Z-L criteria using an average shear stress.
10. One of the major contributions of the EC 2-5 work is the presentation and discussion of data on burst tests of unflawed pipe. These data show that the ratio of burst stress predicted on the basis of uniaxial ultimate tensile strength to actual burst stress increases as much as 10% as the yield/tensile ratio goes from 0.6 to near 1.0. This suggests that failure criteria (including flow stress for simple failure models and limit strain for FE analysis models) for high-strength steels that exhibit low strain-hardening could be quite different from those that characterize more conventional materials.
11. *The EC 2-5 team suggests that a smoother relationship on failure predictions of corroded pipe across all grades could be accomplished when using UTS rather than some function of SMYS. In doing this, they first used the material property data from a database of defect-free burst tests conducted. They concluded that the flow stress defined as SMYS +10 ksi was roughly equivalent to actual UTS-18 ksi. They further showed that if SMTS was used for assessing the vintage pipe database, then the flow stress could be defined as SMTS-10.8 ksi (SMTS being lower than actual UTS). They also showed that the SMTS-10.8 ksi definition gave equivalent results with B31G corroded pipe test data was when using SMYS+10 ksi for flow stress. (Note, the caption for Figure 12 in EC 2-5 is in error and misleading.)*
12. *The subsequent discussion on defect-free pipe burst tests data and their analysis in Figure 14 raises some confusion. In the Figure 14 set of data, the defect-free pipe burst stress is well predicted using actual UTS; see Figure 14(c) in EC 2-5. Since most pipe burst stress design criteria (in many industries) are based on burst pressure being calculated from UTS and the Barlow equation, this makes sense – although there is typically a biaxial increase in flow properties for an end-capped pipe that von Mises yield criterion would say is a factor of 1.14. Furthermore, in Figure 14(b) it shows that the burst stress is about 10 ksi* ***<u>higher</u>*** *than when using the SMTS. Again, this makes sense since SMTS should be lower than actual tensile strength. However, the EC 2-5 authors conclude that the flow stress from this defect-free data is SMTS-10.8 ksi, which they said agrees with their vintage pipe assessment. The problem is that the data in Figure 14(c) really shows that the equivalent flow stress (or reference stress) for the defect-free pipe is SMTS + 10 ksi. There appears to be an error in the sign (+10 ksi versus -10 ksi). Hence this aspect should be examined further.*
13. They also looked at hoop strain as a prediction of failure pressure of corroded pipe. They said that their finite element numerical results provided some valuable insights into the plastic strains especially for the experiments with "nested natural" corrosion flaws, *although the FE mesh was quite coarse and results would be questionable unless a mesh refinement study was conducted.*

14. In EC 2-5 the authors incorrectly implied that brittle fracture initiation could occur in the corroded pipe burst tests on vintage pipes. Work by Maxey and Wilkowski showed the fracture initiation transition temperature is well below that of the fracture propagation transition temperature for older vintage pipes. Furthermore a blunter corrosion flaw makes the fracture initiation transition temperature even lower than a sharp crack [2].

The bottom line is that the B31G/Mod B31G/RSTRENG models have been thoroughly validated for assessing the ductile failure behavior of corrosion-caused metal loss in line-pipe materials up through Grade X65 in pipelines not subjected to extreme external loads. Some additional caveats are in order. The original B31G equation can give excessively conservative predictions of failure pressure for long defects. The Modified B31G equation can be applied just as easily, and does not give excessively conservative predictions of failure pressure for long actual (irregular-shaped) corrosion defects as is the case with the original B31G equation. It is noted however, that both B31G for shorter defects and Modified B31G may give unconservative predictions for the failure pressure levels of uniform-depth defects. This is usually not a problem when predicting failure pressure levels of ***actual*** corrosion anomalies because they are non-uniform in depth. It has been shown that the RSTRENG model gives accurate predictions for uniform-depth defects for material grades up to and including X80. However, on the basis of the defect-free burst test results examined by the Battelle team where the higher-strength materials failed at levels less than predicted based on their ultimate tensile strengths, it undoubtedly will be necessary to modify the definition of flow stress when using RSTRENG or Modified B31G for failure stress predictions with X100 materials. Lastly, it is desirable to evaluate the suitability of the B31G and Modified B31G models for higher grade materials (i.e., X100 and up) by comparing predictions to burst test data on samples of these materials that contain non-uniform depth defects that simulated corrosion-cause metal loss.

***Additional Commentary on the Methodology for Calculation of an Equivalent Flaw Size (Emc$^2$ staff)***

Of specific interest from past work reviewed by Dr. Kiefner is the concept of calculating an equivalent 'idealized' flaw using the actual highly complex 'natural corrosion' measurements shape in order to simplify the B31 suite of analyses (including RSTRENG). These procedures were originally developed by Dr. Kiefner and the late Mr. Willard (Bill) Maxey in the late 1960s, when computational techniques were very limited. For example, the RSTRENG approach in ASME B31G which evolved from the equivalent defect technique and considers $L_1$ and $d_2$ as shown in Figure 4 below to be the equivalent defect to the parabolic flaw. Mr. Maxey came up with the equivalent depth, equal area concept to deal with the rounded-end crack-simulating notches that were used in burst tests before Dr. Kiefner developed his methods for corrosion evaluations. This procedure developed by Maxey used the maximum length and an equivalent depth so the area of the equivalent depth flaw is the same as the actual area. The Modified B31G used $0.85*d_1$ and $L_1$ instead (the B31G parabolic case has a shape factor of 2/3 or 0.666 instead of 0.85). However, note that the shape factor concept in B31G, Modified B31G, as well as the Equivalent Area Method (RSTRENG) use a fractional value on the flaw depth rather than the flaw length.

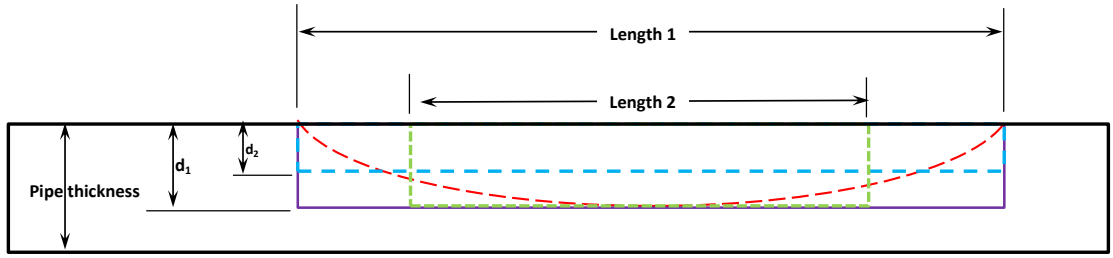


**Figure 4 Sketch showing methods used to calculate equivalent flaw shapes for analyses (Parabolic shape bounded actual flaw shape that is not shown)**

One fundamental question relating to the B31G/Mod/RSTRENG approach is whether the actual length of the corrosion flaw and a calculated equivalent depth (so as to approximate the area of the corrosion) flaw is more accurate, or whether the actual maximum depth with an equivalent length (again the same area of the corrosion flaw) is a better estimate of the "driving force" when relating back to the constant depth axial flaw limit-load equations to calculate a failure pressure. Based on Emc$^2$'s experience from its work in the nuclear industry over the decades [3,4], for circumferential defects in high toughness pipes under axial and bending loads, the actual maximum depth with an equivalent length controls the failure loads (under limit-load conditions). Therefore, to explore an alternative failure criterion, the maximum depth and equivalent length approach was used, as well as the maximum length/maximum depth with shape factor approach. As shown in Figure 5, the equivalent depth assumption (used in the B31G method) will give a higher predicted failure pressure than the maximum depth and equivalent length approach.

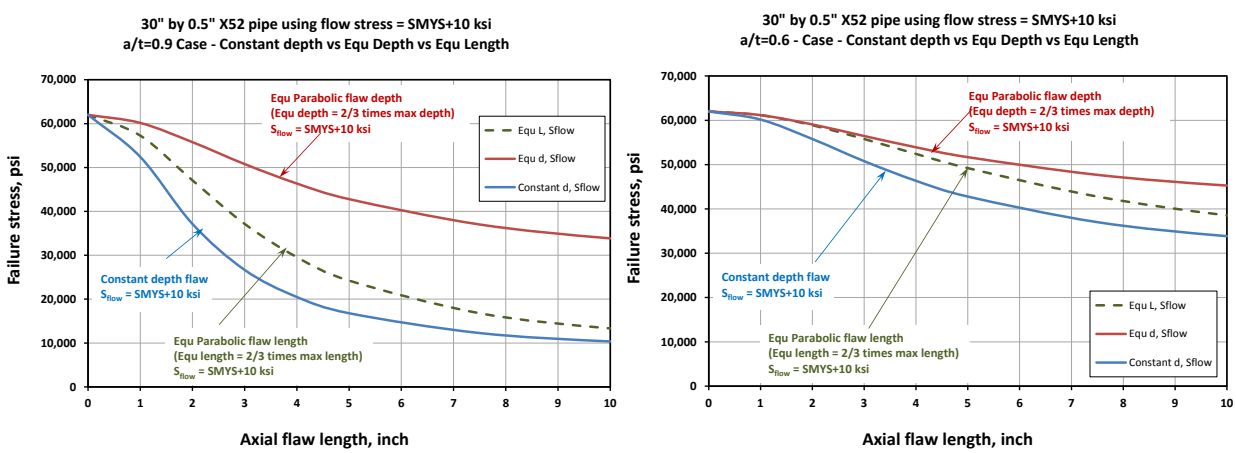


**Figure 5 Failure stress as a function of flaw length for B31G parabolic equivalent depth versus equivalent length approaches for two flaw depths a/t = 0.9 and a/t = 0.6**

To give further credibility to this simple analytical solution, 3D FE analyses were conducted with axial surface flaws of different shape. These analyses involved a 30-inch outside diameter pipe 0.5-inch thick Grade 52 using the stress-strain curve for a 1960 vintage X52 pipe (transverse round-bar tensile test specimen at room temperature and quasi-static loading rates) with various axial surface flaw shapes.

The $Emc^2$ software PipeFracCAE was used to create these FE meshes. The first surface-crack shape had an area of 85% of the maximum depth and length, which is used in Modified B31G analyses assumptions (a 0.85dL case). The maximum depth was 75% of the thickness and the total flaw length was 7 inches. The shape of the flaw was provided by Dr. John Kiefner. PipeFracCAE has an option to make an arbitrary surface crack shape with 40 points, so some nonlinear interpolation was done to make additional points to those defined by Dr. Kiefner, see Figure 6(a).

The second surface flaw had a constant depth of 85% of the maximum value of the variable shape flaw, i.e., a/t=0.75*0.85 = 0.6375; and the length was 7 inches, see Figure 6(b). This is how the Modified B31G analysis determines that a variable shape flaw is transformed to an equivalent constant depth flaw.

The third surface flaw had a constant depth equal to the maximum value of the variable shape flaw, i.e., a/t=0.75; and the length was 85% of 7 inches or 5.95 inches, see Figure 6(c). This is how the nuclear pipe circumferential surface flaw work determines an equivalent constant depth flaw from a variable depth flaw.

The predicted failure pressures by the B31G, Modified B31G, and Effective Area Method (RSTRENG) were calculated by Dr. Kiefner using the KAPA software.

The pressure versus crack-opening displacements in the center of the surface flaw from the nonlinear FE analyses are shown in Figure 7 along with the predicted failure pressures by B31G, Modified B31G, and Effective Area (RSTRENG/KAPA) methods. The FE results were continued to approach what might be the actual maximum pressure, but would need further "nursing" of the analysis to go farther, i.e., changing the convergence criteria in ABAQUS. Nevertheless the last pressure values should be close to the maximum values when using large-strain FE analyses.

There are two key aspects in Figure 7. First the pressure versus COD curve for the actual flaw shape is virtually identical to the constant depth flaw using the <u>equivalent leng</u>th. The equivalent-depth definitions used by the various B31G analyses overpredict the pressure-COD curve from the FE analyses. This is consistent with the variable-shape circumferential surface flaw $Emc^2$ staff has been involved with in the past [3,4].

Secondly, the predicted maximum pressures by B31G, Modified B31G, and Effective Area Methods all underpredict the numerical analyses. This is probably because a flow stress of SMYS+10 ksi was used in the B31G, Modified B31G, and Effective Area Methods, where as a more appropriate flow stress for "true limit-load" behavior may be ultimate strength.

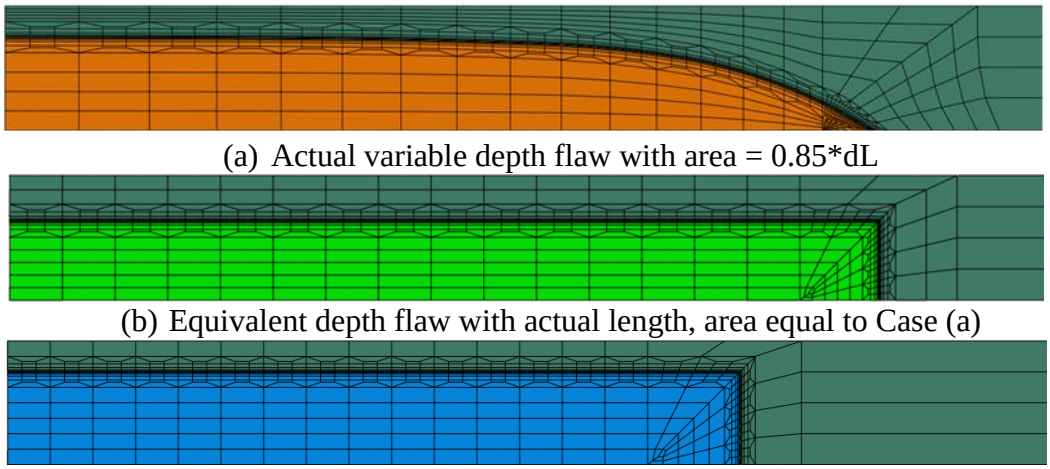

(a) Actual variable depth flaw with area = 0.85*dL

(b) Equivalent depth flaw with actual length, area equal to Case (a)

(c) Equivalent length flaw with actual depth, area equal to Case (a)

**Figure 6 Three FE meshes used for evaluation of equivalent flaw size**

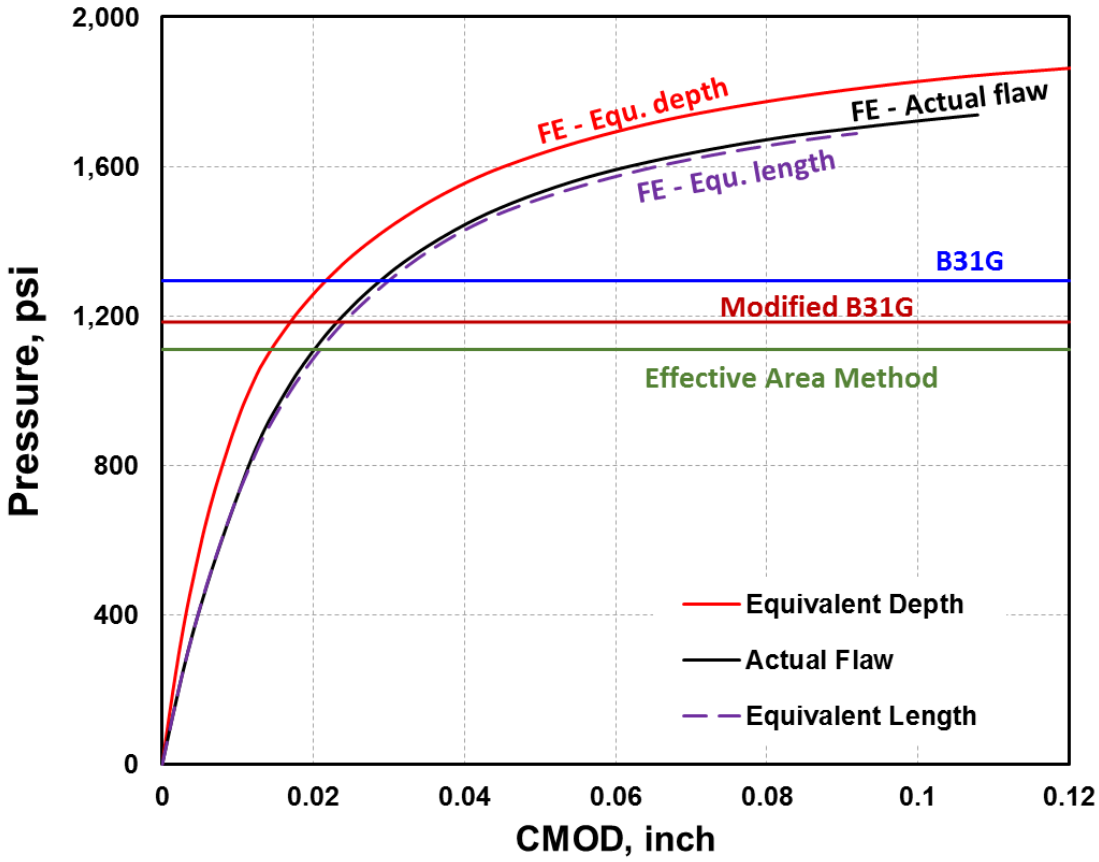


**Figure 7 Comparison of pressure versus center-crack-mouth-opening displacement from the three FE analyses and the B31G, Modified B31G, and Equivalent Area Method predicted failure pressures**

***Summary of Review of Existing Methodologies and Evaluations***

As shown in the review efforts, extensive testing done with corroded pipe as related in the Advantica/GL database shows that the Modified B31G method and RSTRENG are the most accurate of the existing methods for assessing the failure pressure of area of actual corrosion-caused metal loss when using the flow stress definition of SMYS+10 ksi. If the maximum depth and equivalent length from the area of the flaw is used to determine the applied stress more accurately, then perhaps the UTS becomes the more accurate definition of the flow stress; thus giving a better transition between vintage and modern line-pipe failure predictions and ideally lowering the scatter in the test results.

## ***Task 2 – Experiments for Preliminary Failure Criteria for Blunt Flaws***[†]

There were three sets of experiments conducted in this task on specimens machined from two grades of pipe (X52 and X80) that were available in Emc$^2$'s archival storage from previous projects. The X52 pipe was a 36-inch diameter with a 0.39-inch wall thickness, while the X80 pipe was a 48-inch diameter 0.93-inch wall thickness. The three types of specimens tested were:

- Duplicate round-bar tensile tests machined transverse to the axis of the pipe from each of the two materials,
- A single strap tensile test from each material also machined transverse to the pipe axis but first flattened, and
- Six single-edge-notched tensile (SENT) specimens from each of the two materials with an overall notch depth of 50% (a/t =0.5) and six (6) values of notch acuity (notch root radius) to represent various types of corrosion profiles.

***Tensile Test Results***

Figure 8 and Figure 9 show photographs of the round-bar and the strap-tensile tests with standard extensometers used to measure the strain. Figure 10 shows the engineering stress-strain curves from both the round-bar tensile tests from the two materials, and Figure 11 shows the same curves for the strap tensile specimens. As seen, for both materials, the elongation/strain to failure was significantly lower for the strap specimen, whereas the engineering stresses at maximum loads were approximately the same. The lower values of elongation (or strain at failure) for the strap specimen may be attributed to the flattening of the specimen prior to machining which results in some residual plastic strains. Table 5 below provides a summary of the results from the tensile data.

[†] This task was conducted entirely by Emc$^2$ staff.

**Figure 8 Photograph of round-bar specimen under test**

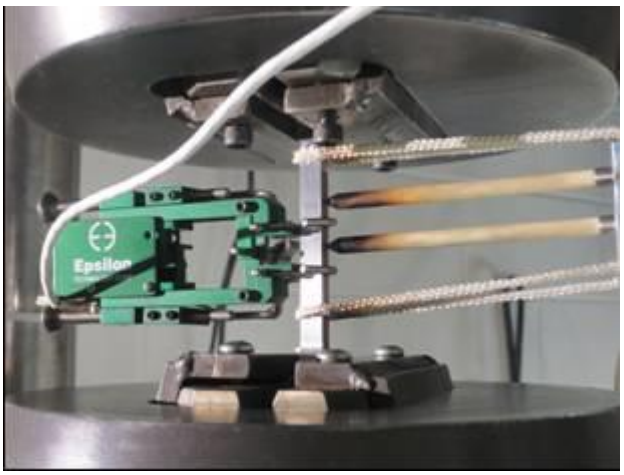


**Figure 9 Photograph of strap-tensile specimen under test**

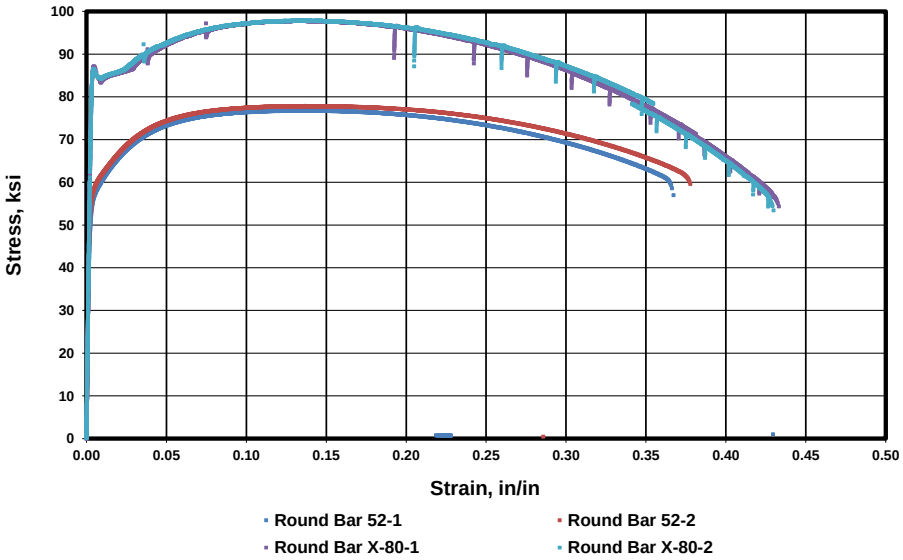


**Figure 10 Engineering stress-strain curves for X52 and X80 transverse round-bar tensile specimens**

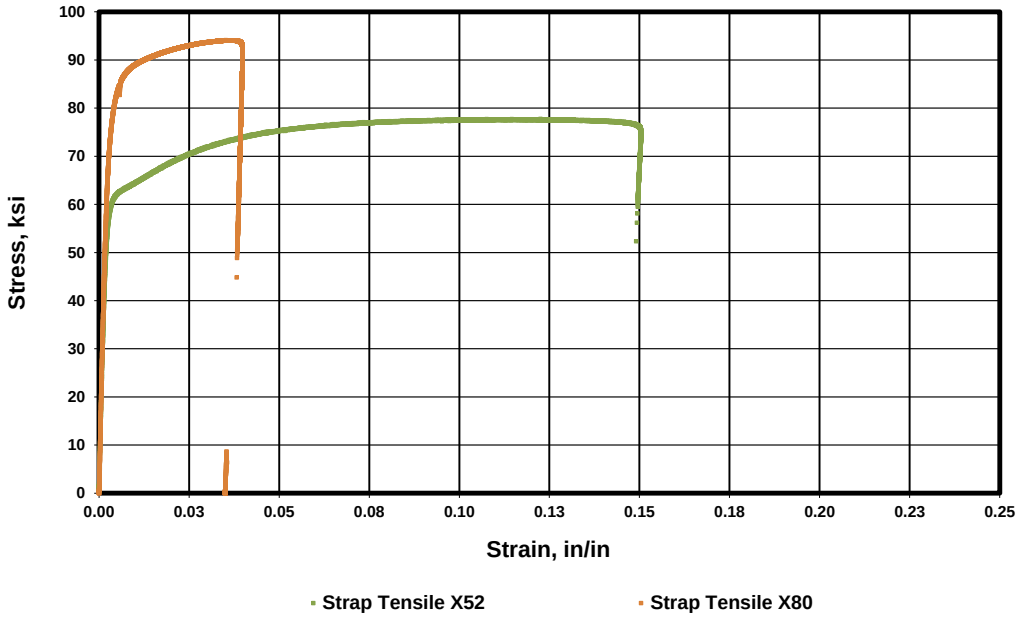


**Figure 11 Engineering stress-strain curves for X52 and X80 flattened-strap transverse tensile specimen**

The material property data from the tensile tests must be further analyzed so that the maximum load can be determined in the nonlinear finite element analysis in modeling the pipe with areal defects. Therefore, the engineering stress-strain curves from the round-bar tensile data were first converted to true-stress versus true-strain curves (to account for cross sectional area changes) and then the true-stress versus plastic-strain curves were developed, shown in Figure 12. These data provide the basis for modeling the yielding and plastic flow of the ligament material associated with areal type corrosion defects in simulating the maximum remaining strength.

**Table 5 Summary of results from tensile tests on X52 and X80 materials (transverse to pipe axis)**

| | Grade X52 | Grade X80 |
|---|---|---|
| Round Bar Specimen | | |
| Yield Stress, ksi | 56.3 | 86.8 |
| Ultimate Stress, ksi | 77.4 | 97.8 |
| Elongation at Failure, % | 25.3 | 27.0 |
| Yield/Ultimate | 0.73 | 0.89 |
| Strip Tensile Specimen | | |
| Ultimate Stress, ksi | 77.9 | 94.2 |
| Elongation at Failure, % | 24.7 | 7.3 |

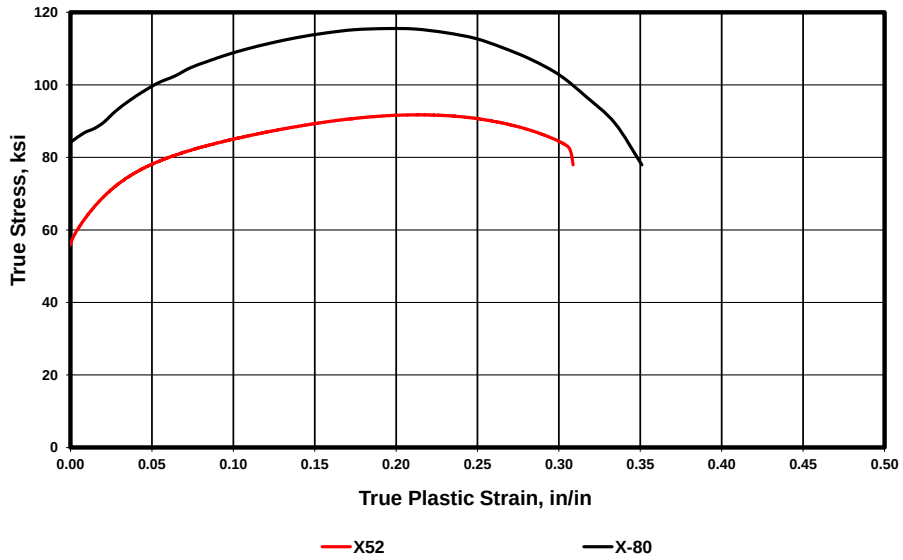


**Figure 12 True stress versus plastic strain curves for X52 and X80 material required as input for the PANC$^2$ methodology**

***SENT Test Results***

A limited set of experiments was conducted in this Phase 1 feasibility study to assess notch-acuity effects on the failure stress of vintage X52 and modern X80 steels. These tests involved SENT specimens with varying notch acuity with the two grades of materials to investigate and confirm the differences in failure mechanism. This is effectively a 2D test of a long surface flaw (without the pipe bulging effect) that is comparable to a ring expansion test. These data will help determine the appropriate failure behavior mechanism and criteria that need to be implemented into the PANC$^2$ methodology for later use in assessing the remaining strength of corroded pipes and fittings with blunt corrosion type areal defects.

Table 6 below shows the dimensions of the SENT specimens used for the X52 and X80 materials. The X52 pipe was also Emc$^2$ Pipe #52 (coincidence with the grade), and the X80 pipe was Emc$^2$ Pipe #753, and happened to also have been used in a previous DOT SBIR Project. Given that the two pipes were of different thickness these dimensions were not identical and we followed the DNV recommended best practice [5] methods for SENT tests as well as Emc$^2$'s experience in SENT testing for over 40 years. Figure 13 shows the set of SENT specimens machined from the 1960 vintage X52 pipe with various notch acuities and blocks welded on to attach clip gages to record the crack-mouth-opening displacements (CMOD) during failure. Figure 14 shows a photograph of a typical SENT specimen under test with two sets of clip gages mounted at different heights from the specimen surface so as to allow the calculation of the CMOD values and also direct-current (d-c) electric-potential (EP) wires attached to the specimen to correctly identify crack initiation during the failure process. During these tests, load, load-line displacement, clip-gage displacements in the two locations as well as the d-c EP were recorded as the SENT tests were conducted at 0.001 inches/second crosshead displacement rate. Each of these tests was completed in five (5) minutes or less.

**Table 6 SENT specimen dimensions for X52 and X80 grade materials**

| Specimen ID | Length | Width | Thickness | Notch Depth | Notch Acuity |
|---|---|---|---|---|---|
| | in | in | in | in | in |
| **Grade X-80** | | | | | |
| X-80-A | 13.9 | 1.269 | 0.835 | 0.4178 | 0.0068 |
| X-80-B | 13.9 | 1.265 | 0.837 | 0.4145 | 0.0130 |
| X-80-C | 13.9 | 1.267 | 0.838 | 0.4163 | 0.0310 |
| X-80-D | 13.9 | 1.269 | 0.836 | 0.4165 | 0.0608 |
| X-80-E | 13.9 | 1.265 | 0.835 | 0.4205 | 0.1253 |
| X-80-F | 13.9 | 1.255 | 0.835 | 0.4213 | 0.2460 |
| | | | | | |
| **Grade X-52** | | | | | |
| X-52-A | 9.0 | 0.485 | 0.323 | 0.1608 | 0.0063 |
| X-52-B | 9.0 | 0.486 | 0.319 | 0.1518 | 0.0153 |
| X-52-C | 9.0 | 0.489 | 0.320 | 0.1610 | 0.0305 |
| X-52-D | 9.0 | 0.481 | 0.326 | 0.1580 | 0.0595 |
| X-52-E | 9.0 | 0.482 | 0.321 | 0.1595 | 0.1238 |
| X-52-F | 9.0 | 0.487 | 0.324 | 0.1553 | 0.2433 |

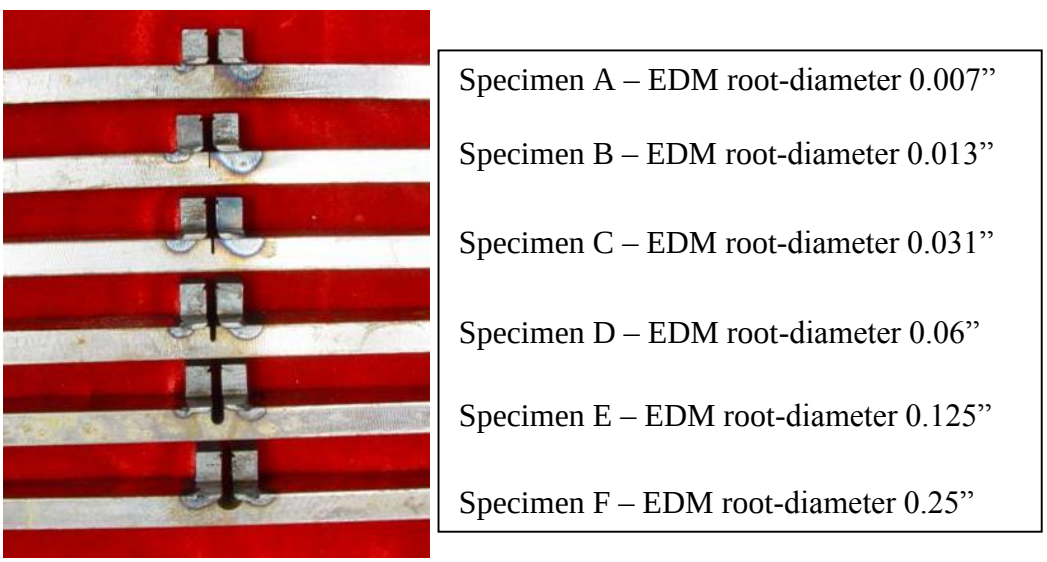


**Figure 13 Photograph of SENT specimens X52-A (sharp) through X52-F (blunt notch) prior to test**

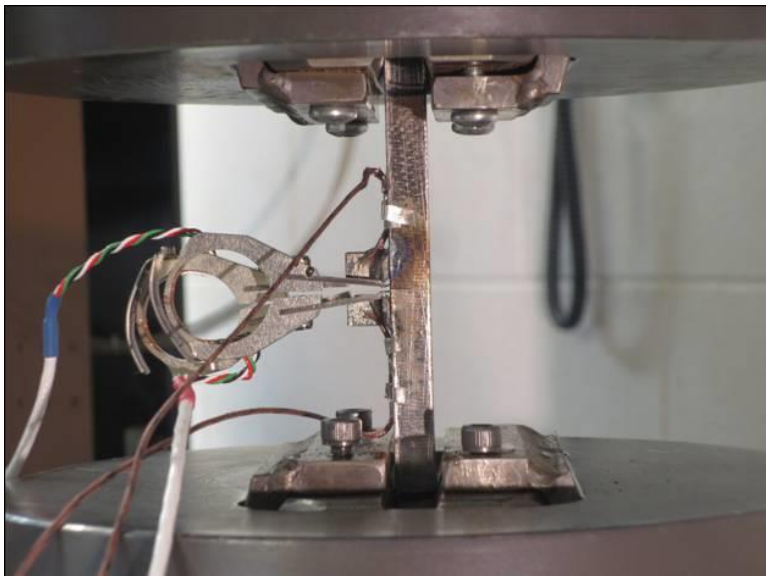

**Figure 14 Photograph of SENT specimen under test showing dual clip gages used to measure CMOD**

Figure 15 and Figure 16 provide the load versus load-line displacement curves for the X80 and X52 materials, respectively. One of the specimens (X52-C) showed anomalous behavior, inconsistent with the rest of the data and was therefore not used in further analysis.

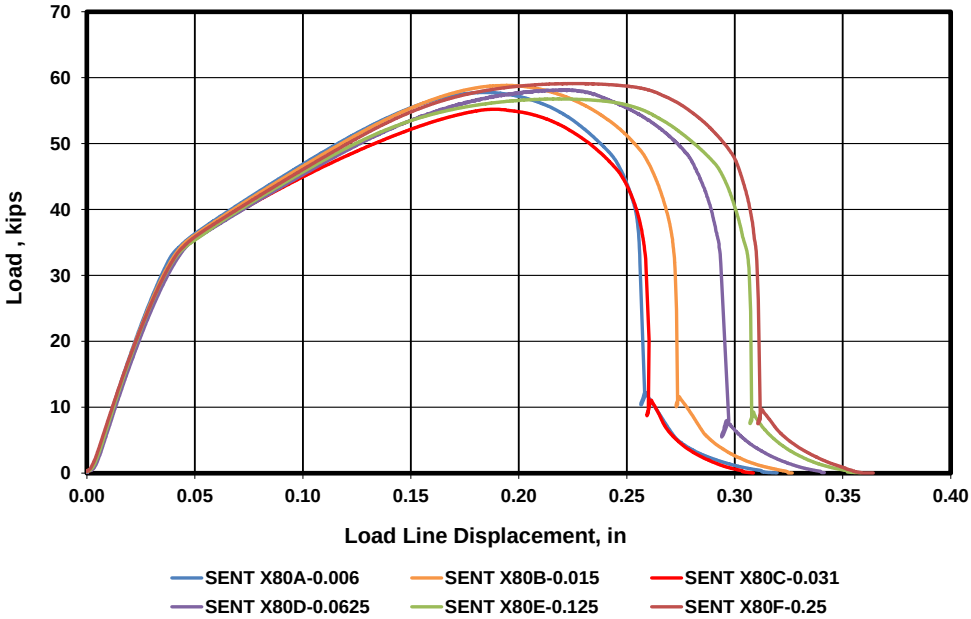


**Figure 15 Load versus load-line displacement for X80 SENT specimens**

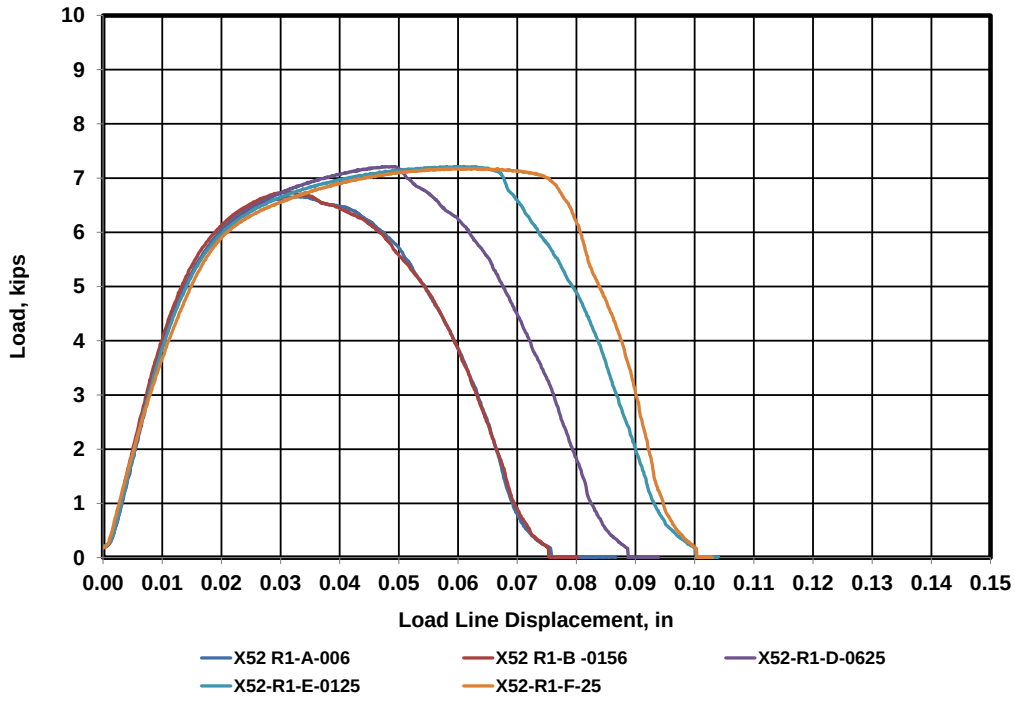


**Figure 16 Load versus load-line displacement for X52 SENT specimens**

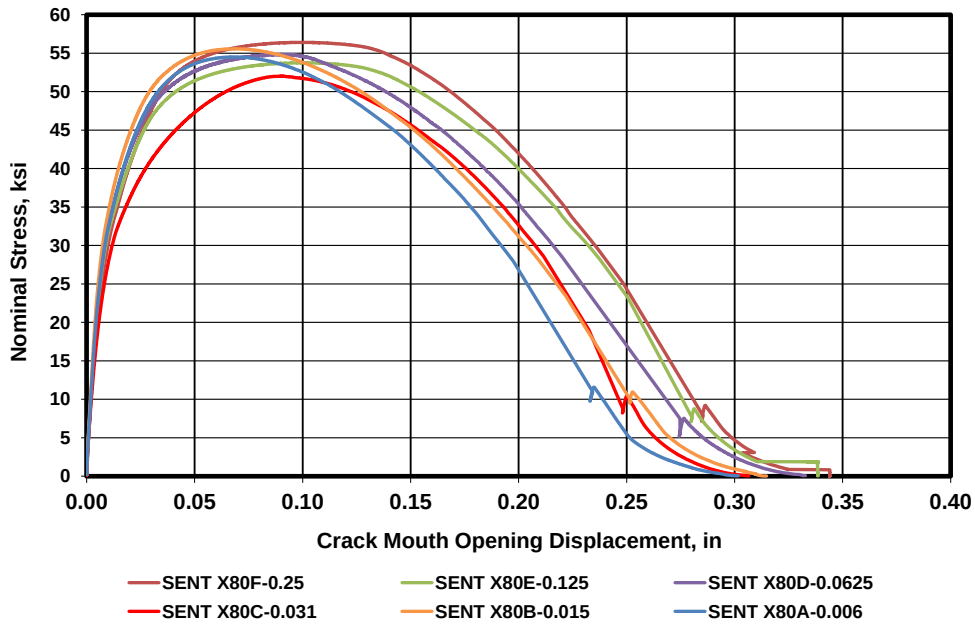


**Figure 17 Nominal stress versus CMOD curves for X80 SENT specimens**

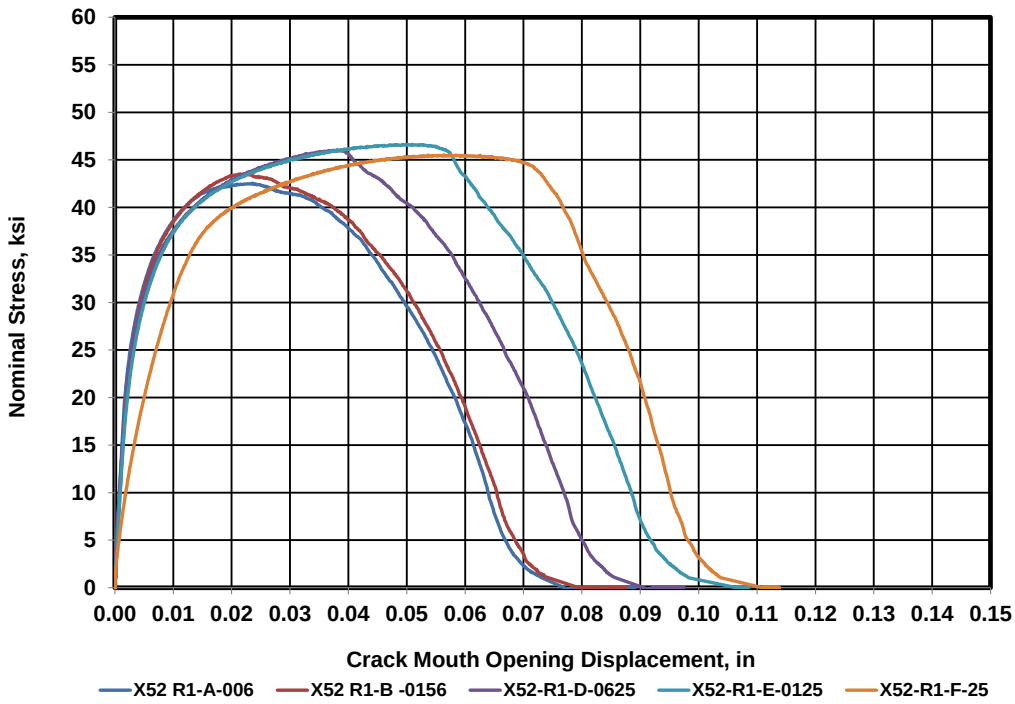


**Figure 18 Nominal stress versus CMOD curves for X52 SENT specimens**

The loads for the X80 specimens are significantly higher than those for X52 primarily because the specimen cross sectional dimensions for X80 are higher as seen in Table 6. Also shown are the nominal stress versus CMOD curves from the two materials in Figure 17 and Figure 18. Crack (or flaw) initiation as measured using the electric potential data [6,7] and maximum load analyses are discussed below along with finite element simulation of the SENT experiments.

These SENT data were carefully reviewed to determine both the effect of notch acuity as well as the material grade on the failure behavior. As seen very clearly in Figure 17 and Figure 18, notch acuity is significantly more important for the vintage X52 pipe as compared with modern X80 pipe. In the former case both the maximum load (nominal stress) and the CMOD at maximum load increases significantly with notch acuity. For the modern higher strength material, this effect is relatively insignificant. Also, the modern X80 steel gets it higher toughness from having lower inclusion content (lower sulphur) than vintage low grade steels (with high sulphur content). However, new X52 steels may also have low sulphur and should behave differently than the vintage X52 steel examined in this effort. Figure 6 above illustrates this conclusion from the experimental data and emphasizes the point that this difference ***MUST*** be accounted for in any failure criteria for assessing the remaining strength of corroded pipeline and fittings in modern line-pipe steels. Also, it must be noted that corrosion flaws could fail under sustained load, and the long duration failure stress might be closer to the load at the start of ductile tearing and not at the maximum primary creep behavior value.

Additional detailed numerical FE analyses of the SENT specimens were also conducted to establish the feasibility of simulating these results for the PANC$^2$ approach as detailed in Task 5.

## ***Task 3 – Leak Versus Break Predictions***[‡]

Per discussions during the kick-off conference web-meeting with the DOT Program Manager and the Emc$^2$ team, this task was given a lower priority during this feasibility study as compared to the other technical Tasks 2, 4, and 5.

From the review in Task 1, for older line-pipe steels the leak versus break boundary can be determined by comparison to the failure pressure for an axial through-wall crack, where the axial crack has the same length as the length of the corrosion flaw.

For modern line-pipe steels, they generally have lower brittle-to-ductile transition temperatures than vintage line-pipe steels; however, they may not be as good as indicated by the Charpy or API standard DWTT. For instance, at -50C a Charpy test can have 400J of energy and 100% shear area, but a fatigue precracked compact tension specimen at 8C had very small amounts of ductile tearing before cleavage fracture [8]. This warmer brittle-to-ductile transition temperature has a huge impact on the leak versus break behavior. Emc$^2$ is working with the API committee on this problem, and has a separate JIP burst testing program, but it is clear that more materials need to be burst tested from that work before a pragmatic modification can be made to the API 5L3 DWTT test procedure.

## ***Task 4 – Precise Assessment of Natural Corrosion via Computation (PANC$^2$) Methodology***[§ ‡]

One of the most critical tasks in this feasibility effort turned out to be developing the PANC$^2$ methodology. This effort starts with the raw data obtained from in-line inspection laser scans of corroded pipes or fittings with the objective of converting them to a finite element mesh for analysis and determination of the remaining strength. For this purpose, Emc$^2$ along with its subcontractor Kiefner & Associates conducted an extensive review of their in-house database of corroded pipe tests or service failures to select a sample case for developing the PANC$^2$ method. Ideally we wanted detailed corrosion profile measurements for a pipe prior to burst testing, the burst test data, tensile test data, and Charpy tests (or chemical analyses). After spending more time than anticipated, we could not find such a well-documented case.

Emc$^2$ then also contacted several pipeline companies to review what data were available from them that involved actual scans of corroded pipe. One major North American company offered to provide a sample case where they had laser scanned surface measurements of a corroded and pitted 36-inch diameter, 0.6-inch wall, X60 pipe.

The laser-measured surface corrosion profile for this sample case was shown previously in Figure 1(a) and formed the starting point for developing the PANC$^2$ breakthrough technology. This corrosion was not very deep, but the meshing procedure also allowed for readily scaling the corrosion depth by any value (hence allowing future corrosion profiles to be estimated). The

---

‡ This task was conducted entirely by Emc$^2$ staff.

§ Originally we called this FE procedure the "Simulation of Natural Corrosion via Computation" (SNC$^2$), but that title was not clear enough to some industry people so it was changed to "Precise Assessment of Natural Corrosion via Computation" (PANC$^2$).

actual corrosion depths from the sample case were magnified by a factor of 4, for the purpose of demonstrating the PANC$^2$ technology as well as the differences between the B31G suite of remaining strength predictions using the X52 and X80 data developed above.

Typically the surface laser scan data as that supplied from the pipeline company are obtained on a 1-mm by 1-mm grid (or grid with 1 mm spacing in axial direction and 2 mm in circumferential direction). The supplier chose to provide it as a standard .STL digital file. The .STL is a public-domain format which represents a surface as a large set of 3-node triangular elements that only follow the corrosion surface geometry. While it is envisioned that the finite element meshing software will import .STL files directly in the future using published ASCII and binary formats, it was convenient in the current effort to use the ABAQUS/CAE (a commercial FE software package) .STL-import facility available at Emc$^2$, for this work. ABAQUS/CAE may be used to automatically write an ASCII *.inp version of .STL files, that is, an ABAQUS input file.

Emc$^2$ also has a proprietary in-house finite-element graphics code developed previously for other complex meshes used to model natural flaw growth of stress-corrosion cracks for nuclear applications. The .STL data received on the above sample case was processed to reveal contours of surface corrosion/pitting (Figure 19). From the green and blue zones it was immediately obvious that the laser scan unit was not perfectly axial to the pipe, so linear regression was applied to restore the data to axiality, which may also be an automated step needed for future Phase 2 work. Gaps in the data were "repaired" by local averaging. Also, an aggregated "river-bottom" profile was extracted from the adjusted data set to run traditional RSTRENG analyses as described in Task 5.

Elastic-plastic finite element analysis places specific requirements on the mesh. It is preferable to use 3-dimensional hexagonal elements and these should be refined in zones of expected plasticity, such as the bottom of the corrosion pits. Focusing on the 60-mm by 60-mm patch around the deepest pit, a cylindrical finite element mesh was generated with refinement in the pit region. The surface nodes of the mesh were mapped to the triangular .STL data. Figure 20 shows the resulting finite element ring mesh when the measured corrosion is accentuated by four times. The 59% loss of section is shown in Figure 21.

For accuracy, it is essential to ensure that model restraints and axial tension loads are remote from the pit region so the mesh is extended by three diameters in each direction. In practice, a 400-mm by 400-mm zone was mapped to the .STL data and this zone was surrounded by a 100-mm linear transition to full thickness (Figure 22). With 300,000 elements, this mesh is relatively large and will benefit from techniques to economize on the number of elements in the periphery.

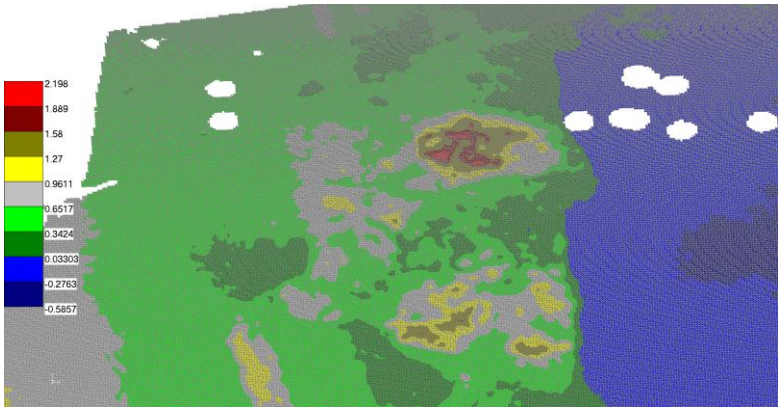


**Figure 19 Details of surface corrosion/pitting contours (as-received data)**

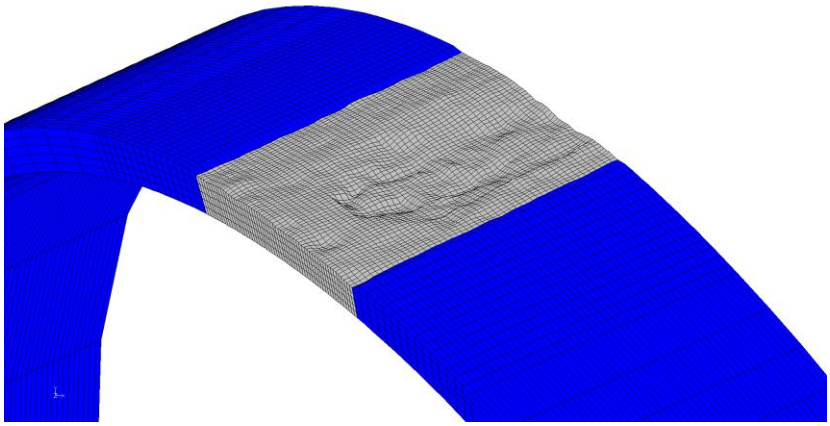

**Figure 20 Finite element ring mesh of 60-mm by 60-mm pit region**

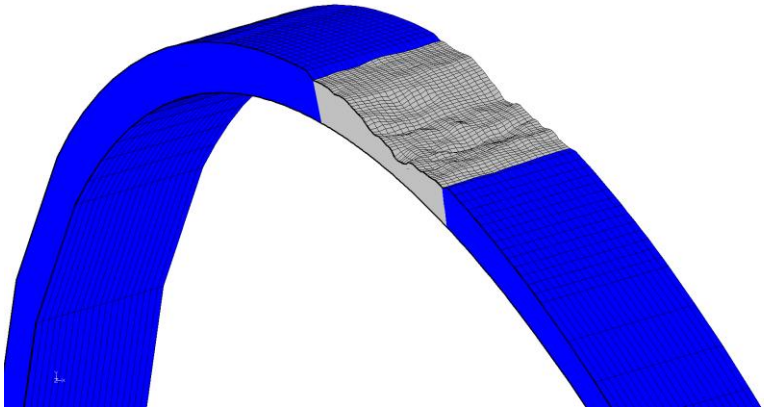

**Figure 21 Section showing 59-percent loss of thickness**

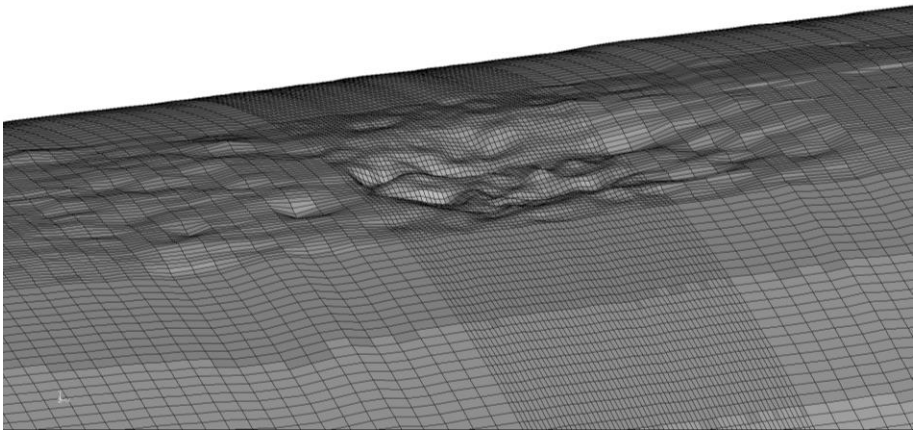

**Figure 22 Mesh with 400-mm by 400-mm corroded region and linear transition to full thickness; also shown in Figure 1(b)**

## ***Task 5 –Feasibility of Precise Analysis of Natural Corrosion via Computation PANC$^2$ Approach****

***Finite Element Analysis of X80 and X52 SENT Specimens***

The very first step in the feasibility of the PANC$^2$ approach is to be able to simulate the laboratory coupon results of the SENT tests using the tensile material properties for each of the two grades of material used. Detailed 3D FE meshes were generated for three cases of notch acuities -A, -D and -F for X80 and -A, -D and -E for X52 in Table 6 representing the sharpest notch (crack), blunter notch or localized pit, and the bluntest notch used, respectively. Given the budgetary constraints of the Phase 1 effort, only 3 of 6 specimens were analyzed for each grade to demonstrate feasibility of this approach. Figure 23 shows these meshes for the X52-A, X52-D and X52-E specimens.

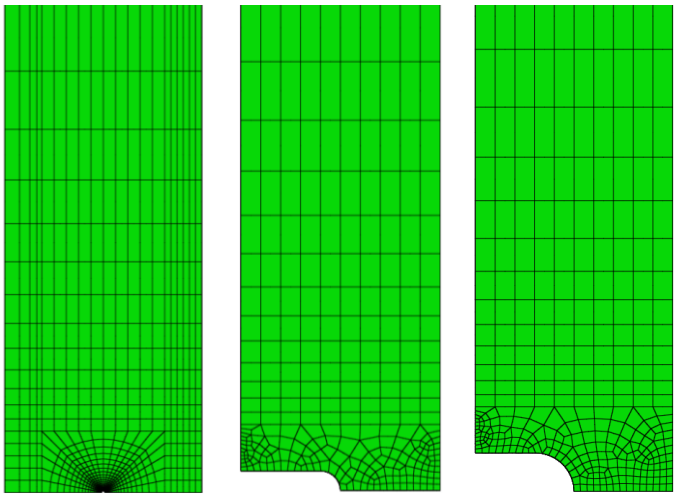


**Figure 23 FE meshes for the X52A, X52D, and X52E specimens**

** This task was conducted entirely by Emc$^2$ staff.

A detailed quarter-symmetry FE mesh for the X-52D case is shown in Figure 24 along with the two planes of symmetry.

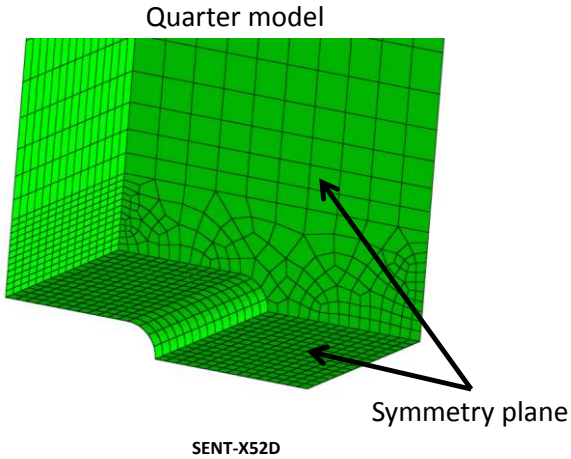


**Figure 24 Quarter-symmetry FE mesh for SENT-X52D showing planes of symmetry**

Figure 25 below shows the FE mesh for the SENT X80-F case superimposed on a photograph of the actual specimen demonstrating the accurate representation of the specimen geometry and notch acuity in the FE simulation work conducted.

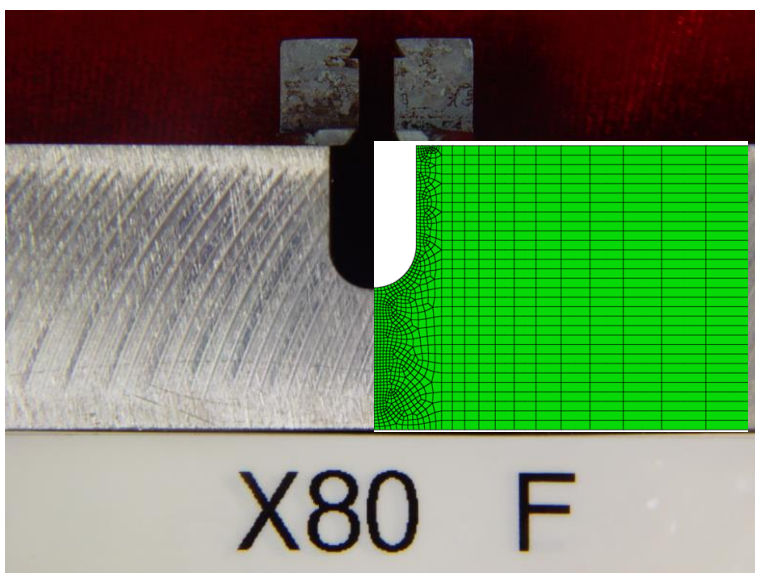


**Figure 25 FE mesh for SENTX80-F superimposed on photograph of specimen**

The next step involved using the true stress versus plastic strain data obtained from the round-bar tensile tests, shown in Figure 7, for the two grades to simulate the SENT specimen results – specifically the load versus crack-mouth-opening displacements (CMOD) data. Figure 26 shows the numerically predicted load versus CMOD curve for the SENT specimens as compared to the actual data from the three X80 specimens. For clarity, the exact value of crack initiation in the SENT experiments determined using the d-c electric potential drop method is also shown in Figure 27. As can be seen the FE prediction is almost exact for these cases all the way up to

crack initiation, but it is important to note that there is no crack growth modelling in the FE analyses or other failure criterion other than development of tensile necking instability in the SENT blunt notch specimens. The simulation of crack growth beyond initiation using damage mechanics models [9] or other crack propagation models was beyond the scope of the Phase 1 effort and will be undertaken in the Phase II effort as appropriate. The numerically predicted curves with no failure criteria do not follow the actual specimen behavior beyond maximum load as seen in Figure 26 since crack growth was not included.

Pragmatically, once the ductile tearing starts to occur, the flawed pipe/specimen is relatively close to the maximum load. Since real corrosion flaws in pipe are in a load-controlled state and the pressure is maintained in a gas line for long time periods, there is the likelihood that there would be primary creep (or sustained-load crack growth) to failure at the pressure/stress where the ductile tearing starts. Many studies on sustained-load crack growth have been conducted with sharper flaws [6,10], but the blunter flaws in the SENT tests in this project show ductile tearing prior to reaching maximum load. This might be the more important failure criterion that is needed.

Additionally, from these analyses it can be seen that using a FE analysis with a corrosion flaw and trying to predict the maximum pressure capacity can give an over prediction of the actual maximum failure stress (pressure). This methodology is generally allowed in B31G Level 3 analysis [11], but they recognize that, *"A failure criterion should be developed that considers the strain capacity or fracture resistance characteristics of the material."*

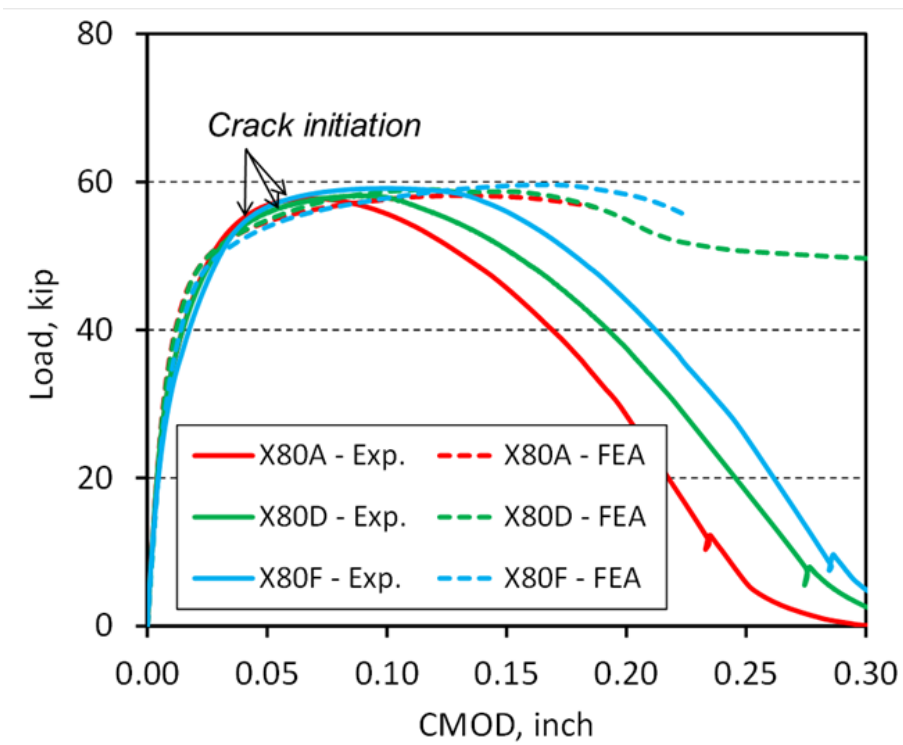


**Figure 26 FE predictions and actual load versus CMOD curves for SENT specimens X80-A, X80-D, and X80-F specimens (no crack growth in FE analyses)**

Similar analyses were also conducted for three of the X52 SENT specimens X52-A, X52-D, and X52-E and these results are shown in Figure 27 below. The numerical load predictions are below loads in the experimental curves for each of these cases up to crack initiation, even though the initial slope of the curves until yield is followed exactly. The likely explanation for this difference is the result of flattening the SENT specimens before testing that result in strain hardening the steel, which may be more significant for the X52 materials than the X80 materials. Such anomalies between lower and higher strength steels must be addressed and resolved during a follow on Phase 2 effort and accounted for in any failure criterion for the pressurized pipe or fitting.

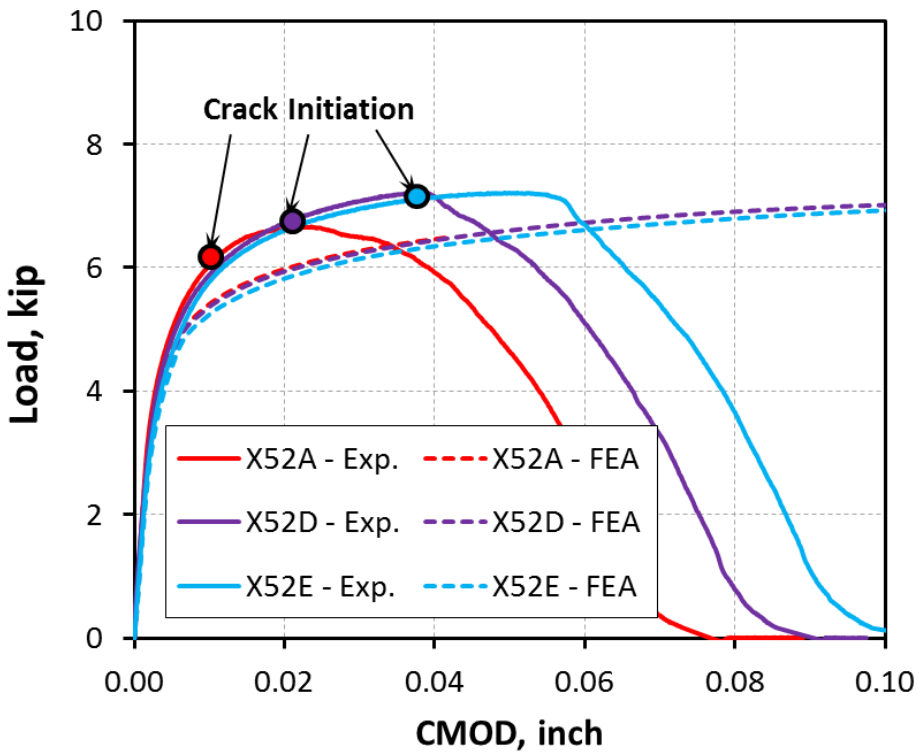


**Figure 27 FE predictions and actual load versus CMOD curves for SENT specimens X52A, X52D, and X52E**

***<u>Finite Element Analysis of Sample Case of Corroded Pipe Specimen</u>***

The final step in the PANC$^2$ approach during Phase 1 was to confirm that the FE mesh created to simulate the natural corrosion defect using the sample case described in Task 4 could run on a commercial software package as well as on an open source FE package on a supercomputer system based in the 'Cloud' which would be the eventual commercial product from Phase 2 of this effort.

The FE mesh developed from the proprietary software to simulate natural corrosion flaws described above was first exported to a format that could be directly imported into the commercial software package ABAQUS. This was successfully done following which both geometrical constraints and pressure loading conditions on the pipe segment were applied using standard procedures. Unlike the case of the SENT specimens that involved displacement-

controlled loading, the sample case of the pipe under pressure is in load control. The material property data for the X80 grade (true-stress versus plastic strain from Figure 7), were provided as input for this sample case. Since no experimental data are available for comparison to the FE predictions for this flaw geometry/material case only the stress distribution can be reviewed for consistency, especially in the plastic strain region. (Such full-scale instrumented pipe burst data involving natural corrosion defects will be conducted in and available in Phase 2 to fully validate the PANC$^2$ methodology). Meanwhile, during this phase of the work, the effective or Von Mises stress contours were reviewed in various regions of the corrosion profile for the sample case. Figure 28, Figure 29, Figure 30, and Figure 31 show various results from the ABAQUS FE analyses confirming that the natural corrosion profile from the PANC$^2$ methodology results in no numerical instabilities or problems when coupled with standard commercial software packages such as ABAQUS.

For comparison to the B31-type analyses, it is desirable to assess how high the pressure may be in this FE model even if the failure criterion is not fully developed yet. In this model we included the strain hardening of the material, but since this is a load-controlled (pressure) problem, it not possible for the FE solver to calculate when the pressure level drops, i.e., it will just stop being able to solve the problem. If one assumes the material is elastic-perfectly plastic (no strain-hardening) then a methodology called a Riks analysis can be used to go beyond maximum load/pressure. However, the Riks type analysis although of some guidance, is not as desirable as including the strain-hardening. So ideally there is a failure criterion in the future that overcomes the current ability in pressure loading to know if maximum pressure is actually reached. Nevertheless, to examine the results of the FE analysis in this case, the pressure was plotted as a function of the circumferential displacement of node points either side of the worst location in the corroded region. This is effectively like an opening displacement across the flaw. This pressure versus displacement plot is shown in Figure 32, which shows the highest calculated pressure is probably close to the failure pressure, but still lower than if localized necking occurred, i.e., true limit-load behavior reached.

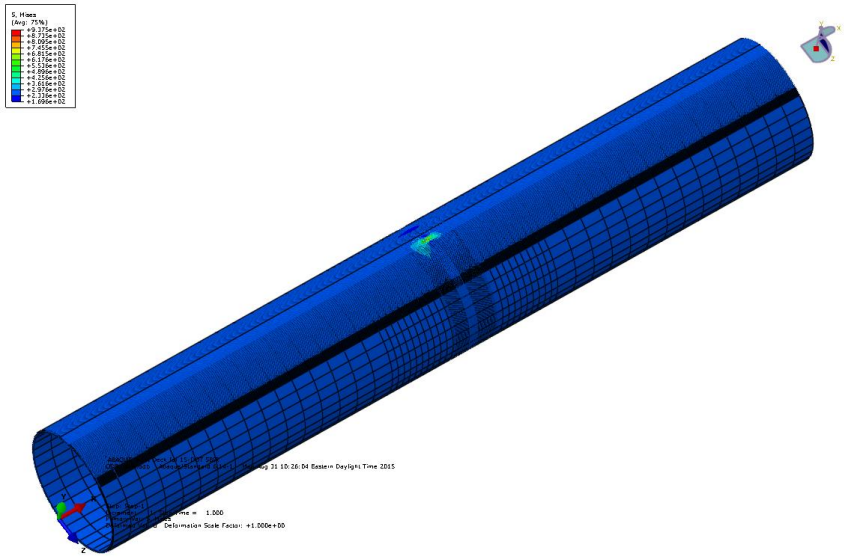

**Figure 28 Overview of pipe FE mesh showing corrosion profile for the sample case analyzed**

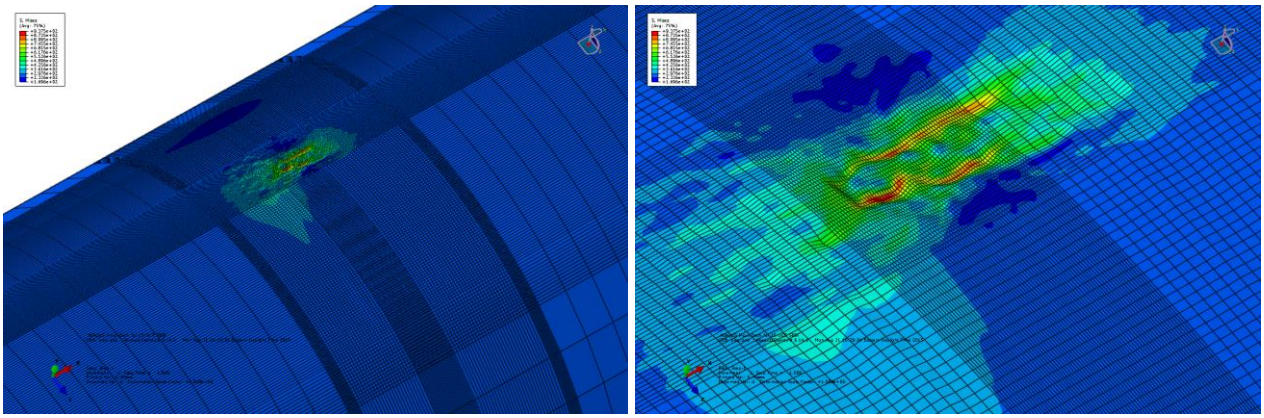

**Figure 29 Close up of ABAQUS von Mises stress contours in the corrosion profile**

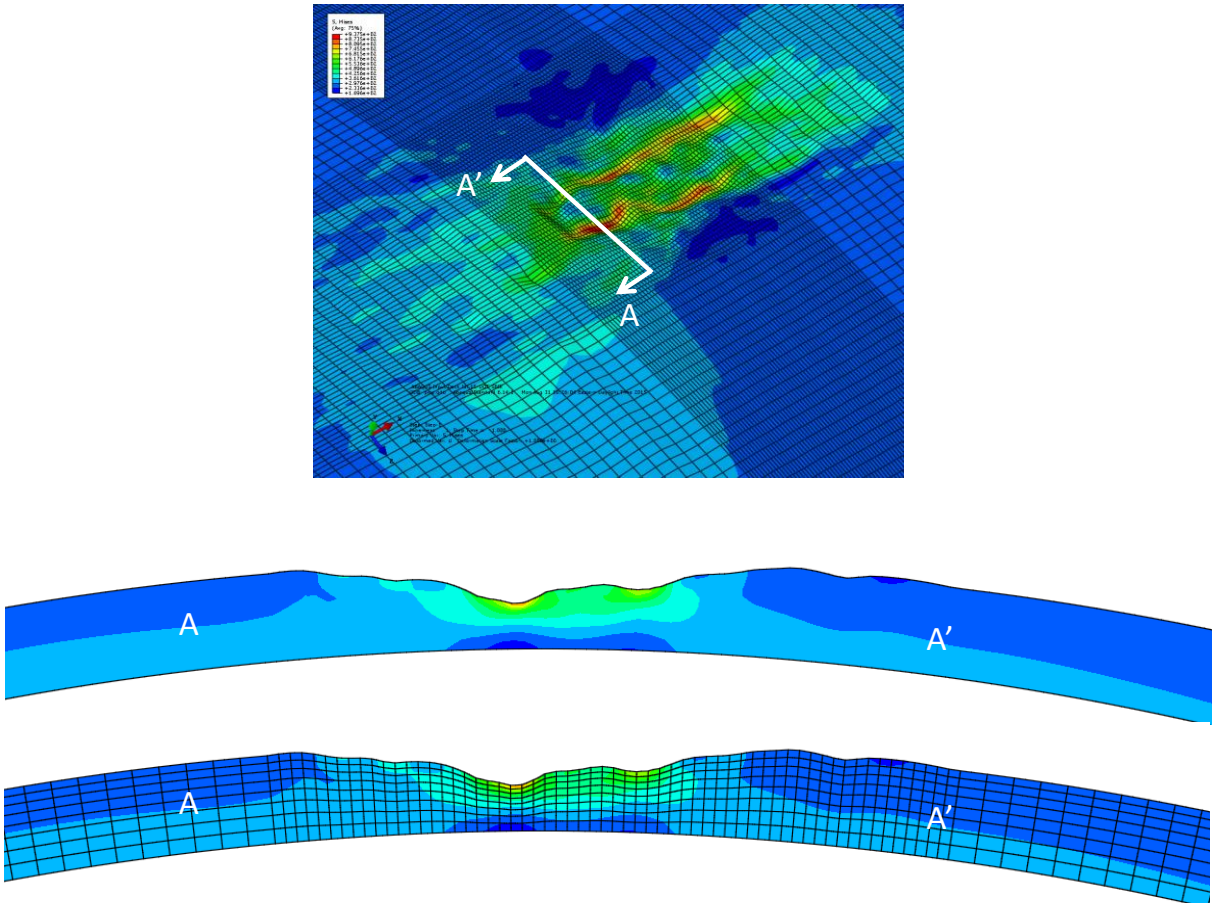


**Figure 30 ABAQUS von Mises stress contours at Section A-A' of the corrosion profile**

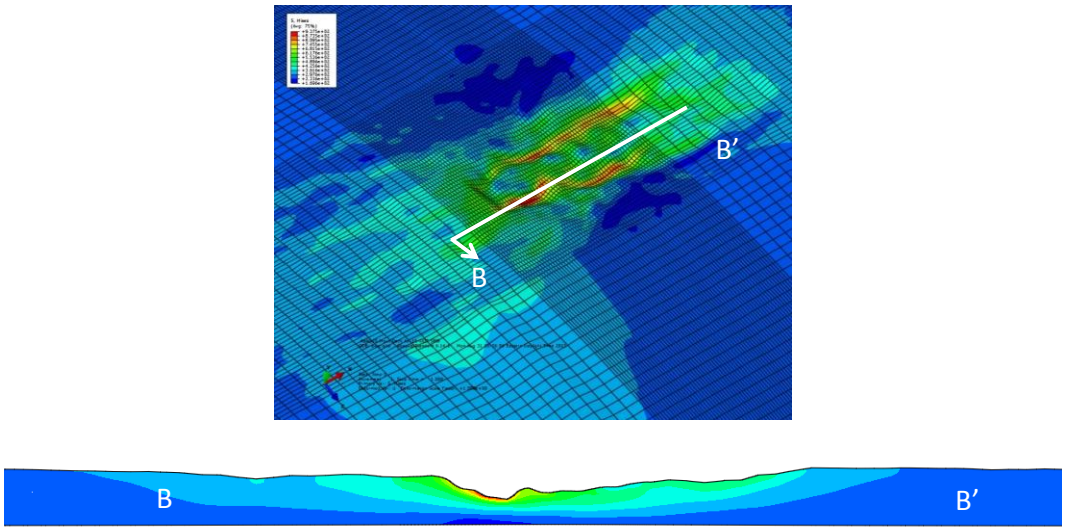


**Figure 31 ABAQUS von Mises stress contours at Section B-B' of the corrosion profile**

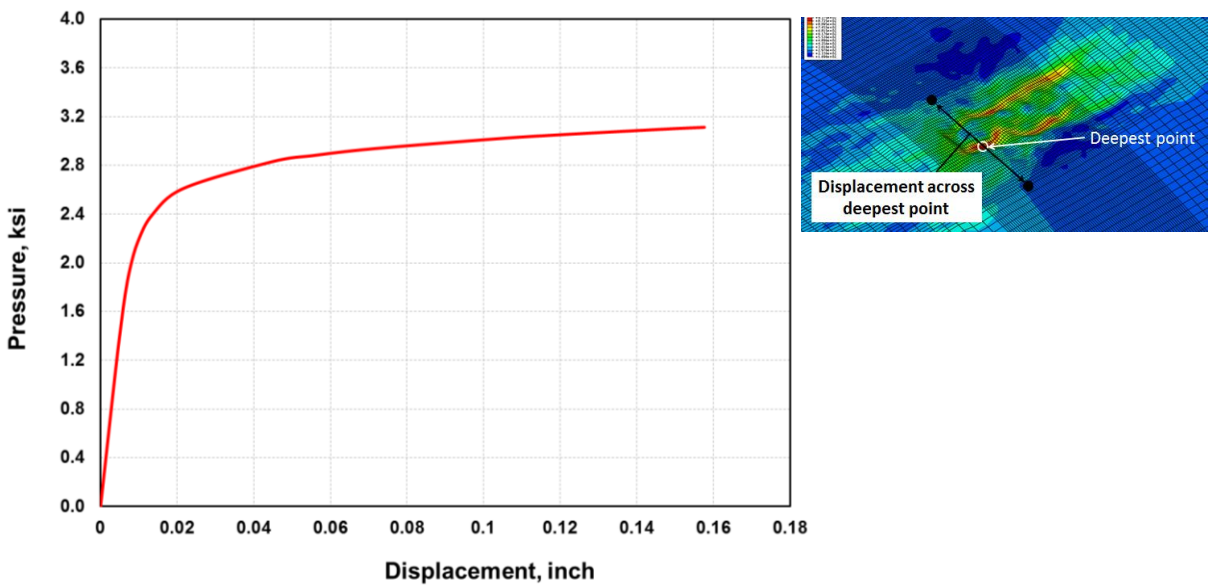


**Figure 32 Pressure versus displacement across the nodes at the highest stresses axial location along the corrosion profile from ABAQUS FE analysis**

The last aspect of the feasibility study involved converting the FE mesh from PANC$^2$ used in ABAQUS to the open source WARP3D FE program modified by Emc$^2$ and hosted at the Ohio Supercomputer Center (OSC) at The Ohio State University (OSU). The WARP3D software will be used instead of ABAQUS since it is open-source software with no licensing restrictions like ABAQUS. Under a separate contract Emc$^2$ has developed a robust high-performance computational (HPC) Virtual Fabrication Technology (VFT) finite element code for commercial application of welded structure fabrication and prediction of distortion, warping, and residual stresses prior to actual welding and manufacture of heavy-walled structures. The heart of that software is an updated version of the WARP3D FE analysis solver. Since the overall goal of this

SBIR project is to make the PANC$^2$ methodology available on the 'Cloud' through a hosting supercomputer facility, the input file for ABAQUS for the above sample case was also converted to the format required for WARP3D FE software. The case was run on OSC's Ruby supercomputer platform [12] to establish that the platform could handle the type of mesh in PANC$^2$ and determine the increase in speed and efficiency of using this method in Phase 2. (Ruby has up to 240 nodes each with 20 processors compared to Emc$^2$ servers with 12 processors.) For this simple demonstration problem the 'wall time' using WARP3D was almost 6 times faster even without using the full computational capabilities of the OSC (only 20 processors were used while up to 80 are available to be run in parallel for large numerical simulation problems). Also, a much larger supercomputer cluster than Ruby is currently being built at the OSC, so the CPU time will be further reduced by the time the Phase 2 software is available for public use.

A comparison of the ABAQUS versus WARP3D FE solutions using the X52 and X80 stress-strain curves is shown in Figure 33, where the pressure steps were identical in the ABAQUS and WARP3D runs. The results are very comparable showing that WARP3D can be used in the future Cloud-based software.

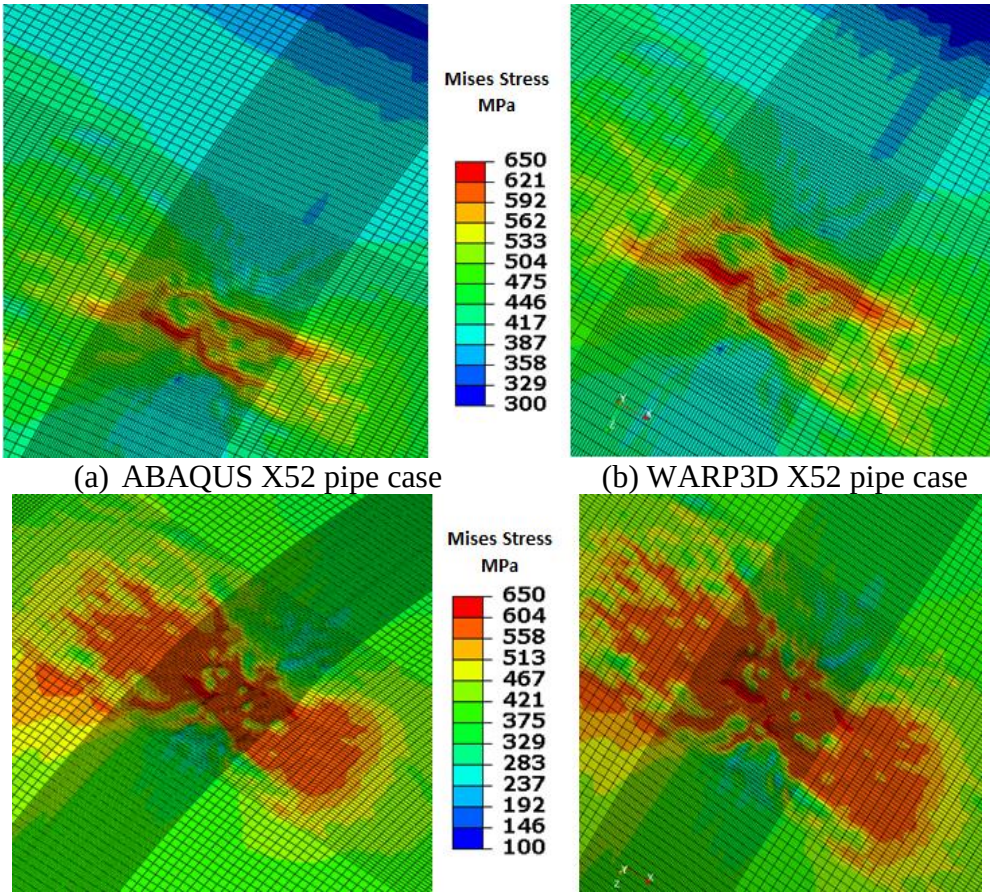


(a) ABAQUS X52 pipe case (b) WARP3D X52 pipe case

(c) ABAQUS X80 pipe case (d) WARP3D X80 pipe case

**Figure 33 Comparison of ABAQUS and WARP-3D FE results at identical pressure steps**

***B31G-Type Analyses Failure Predictions of Sample Case***

As a follow up to the work in Task 1 summarizing existing methodologies, the sample case above was also analyzed using the publically available KAPA program from Kiefner & Associates [13] for completeness. KAPA is based on the same basic analytical approaches described in the most recent revision of ASME B31G [11] and provides a failure pressure prediction given the corrosion profile (as a "River-bottom") along with the pipe diameter, wall thickness, and grade. No other information is required for this semi-empirical approach originally developed in the 1970s and summarized in Attachment 1. KAPA has been validated against the commercial software code RSTRENG by Kiefner & Associates whose staff were also involved in this activity. The "River-bottom profile" for the sample case was extracted from the FE mesh as indicated in Task 4 and is shown in Figure 34 below. The input values for this sample case were used to predict the failure pressure for the three cases in KAPA; (i) Original B31G, (ii) Modified B31G, and (iii) Effective Area Method (RSTRENG) and are shown in Table 7.

A comparison of these values to the ABAQUS X80 FE results is shown in Figure 35. The FE analysis is preliminary since there is no failure criterion established for it yet; however if the failure was true limit-load by necking instability, the maximum pressure from the FE run is conservative. Additionally as mentioned earlier, since this is a load-controlled analysis the pressure values could be increasing further by tightening up the convergence criteria. The shape of the FE load-opening displacement across the nodes at the deepest location gives some idea of how close to the maximum pressure the FE analysis was run. These results show that the B31G-type analyses, all using flow stress of SMYS+10 ksi seem conservative for this flaw geometry. The scatter of the failure pressure predictions for the B31G-type analyses for this very irregular flaw shape is much greater than the smooth flaw examined in Task 1, see Figure 6. Of course, this result is from only one flaw geometry, so the trends between the B31G-type analyses and the FE results might change with other irregular flaw cases.

Interestingly, the Effective Area Method for this very irregular flaw geometry gave higher failure pressures than B31G or Modified B31G. This is the opposite trend from the smooth flaw shape evaluated at the end of Task 1, see Figure 7.

Also as noted at the end of Task 1, using an effective length with a maximum depth (rather than the actual length and effective depth) in combination with the material ultimate strength may improve the accuracy of the various B31G-type analyses failure predictions, or give more consistency to the trends.

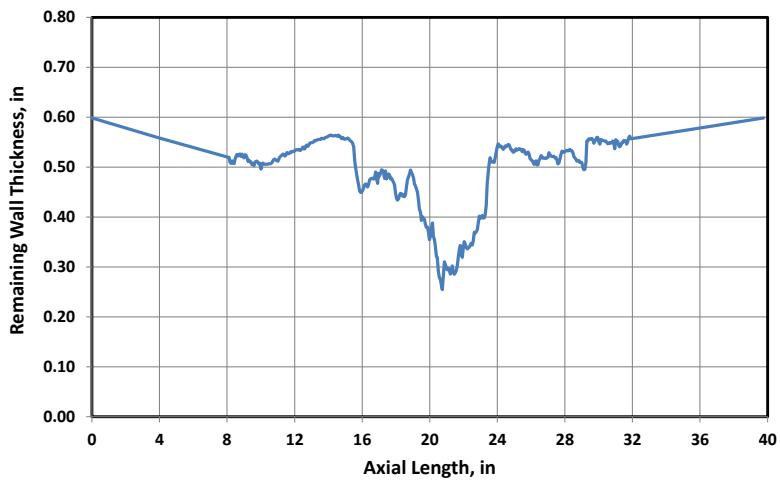


**Figure 34 "River-bottom" corrosion profile for 36-inch diameter 0.600-inch thick pipe sample case above used in B31G-type analyses**

**Table 7 Predicted failure pressure using RSTRENG type analyses**

| Analysis Method | X52 failure pressure, psig | X80 failure pressure, psi |
|---|---|---|
| B31G | 809 | 1,245 |
| Modified B31G | 1,154 | 1,675 |
| Effective area method (RSTRENG) | 1,728 | 2,509 |

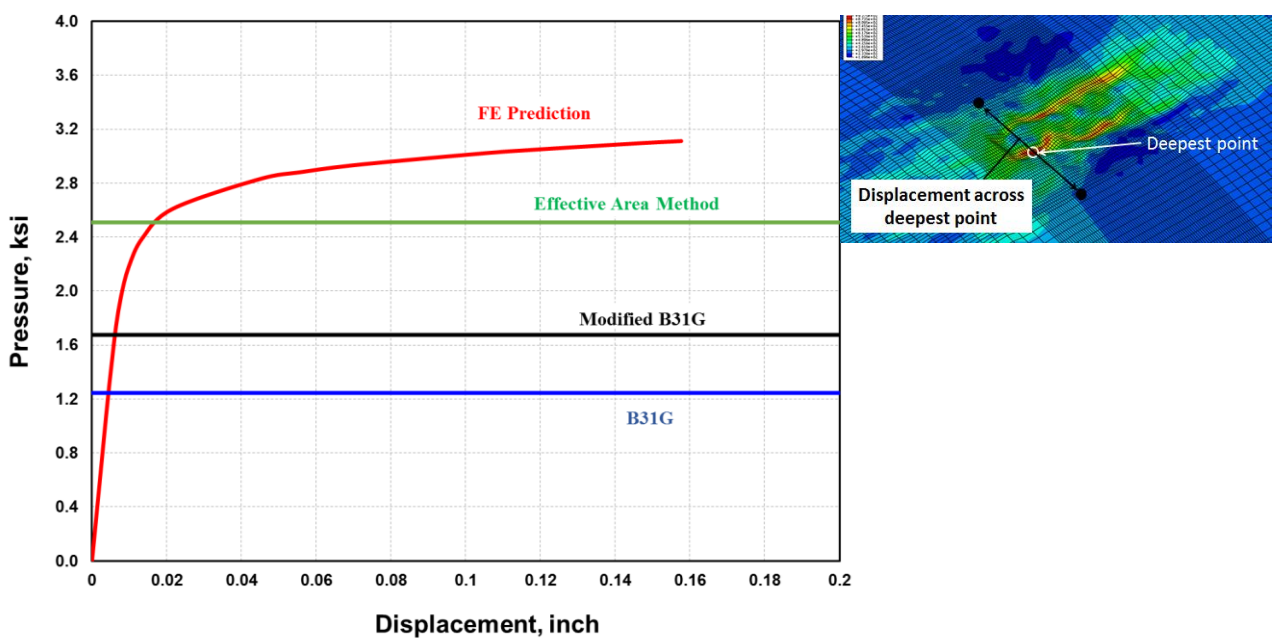


**Figure 35 Comparison of B31-type predictions to ABAQUS FE results for the X80 case (B31-type analyses used flow stress = SMYS +10 ksi)**

***Approaches to Implementing Failure Criteria into PANC$^2$ Methodology***

While developing the PANC$^2$ methodology and establishing its feasibility was the main accomplishment of this Phase 1 effort, an equally critical finding from the experiments conducted was that modern higher strength steels such as X80 show very different failure behavior than vintage X52 materials at various notch acuities – such as those present in large corroded profiles in pipes and fittings. The higher grade material tested was less sensitive to notch acuity as shown in Figure 2 since the CMOD does not increase significantly with increase in notch tip radii. It is also possible that modern X52 steel will have higher toughness (most steels now have lower sulphur that increases the Charpy energy considerably) and behave closer to the X80 pipe tested here. This fact is not accounted for in the traditional approach described above, which only takes into account the strength and the equivalent flaw depth profile in predicting the failure pressure and thereby the safety factor.

A more precise failure criterion for the modern line-pipe steels (low and higher grades) will require additional laboratory and pipe burst test data so that it can be implemented into the PANC$^2$ FE methodology.

# Task 6 – Program Management, Coordination, Reporting, and Travel

The activities in this task included coordination and management of the various tasks with the subcontractors and other partners such as the pipeline company that provided some of the data from actual pipe scans needed in this effort. Specifically the activities in the task involved the following:

i. Preparing and submitting a Technical Brief
ii. Conducting a 'kick-off' conference call with the DOT-PHMSA COR, Emc$^2$ staff, PRCI, TransCanada (TCPL) and other industry representatives
iii. Preparing and submitting the Interim Progress Report – 1
iv. Preparing and submitting the Interim Progress Report – 2
v. Conducting a web meeting with TCPL that has been very interested and supportive of this effort. Specifically, extensive discussions were held with their technical and research staff including Mr. Deli Yu, Mr. Richard Kania, and Mr. David Weaver. As a result of these discussions, TCPL has committed to support this project as a strategic partner both during the Phase 1 and the Phase 2 project, when undertaken.
vi. Providing periodic updates (via email and conference calls) on the technical progress in various tasks on this project to the COR.

For the Phase 1 effort, only local travel was needed.

No significant technical challenges were encountered during the Phase 1 effort. However, there were some delays in both procuring and machining specimens for the experimental work, and therefore a three-month, no-cost time extension was requested to complete the project successfully.

# DESCRIPTION AND SCHEDULE OF FUTURE WORK NEEDED FOR FURTHER DEVELOPMENT

Based on the successful Phase 1 feasibility study results detailed above, Emc$^2$ proposes that the following work be undertaken in the future Phase 2 project. These tasks below are identified as recommendations to the Government in assisting in the development of future work in this contract.

***Automation of the PANC$^2$ Methodology:***

The feasibility of creating natural corrosion meshes from scanned field data of corroded pipes and fittings was established in Phase 1 in preparation for the Phase 2 effort. During Phase 1 a semi-automated method was used to create an FE mesh to simulate corrosion defects in piping. For commercial, real-time application of this technology a fully automated mesh generation software that takes as its input any corrosion profile data file in a .STL (or other similar format) and converts it to a full, 3-dimensional, 20-noded brick finite element mesh will be needed for accurate assessment of the remaining strength. Furthermore, a 'gravity-assisted' approach for mesh refinement in the corrosion regions of the pipes and fittings will need to be perfected as part of the automation process so the mesh density is greater in critical areas and the simulation will provide more accurate results. The development and implementation of such a PANC$^2$ mesh generator hosted in the 'Cloud' on a supercomputer platform will be one of the primary goals during the first year of the Phase 2 project.

Although not fully implemented into the pipe FE meshing routine, a mesh refinement procedure was developed so that if measurements were not made on a fine enough grid, then it is possible to slide or focus more nodes in the deeper locations. Figure 36 illustrates this node sliding methodology.

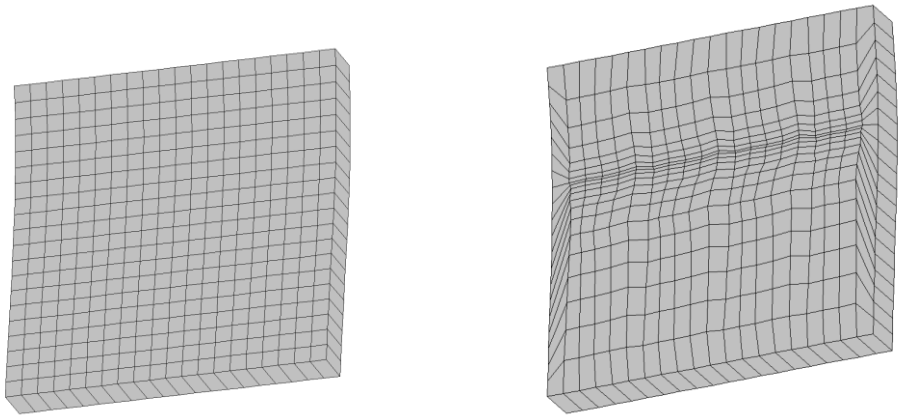

(a) Grid that measurements are made (b) Grid after inserting a "corroded region" and nodes slid to deepest location

**Figure 36 Illustration of node-sliding methodology for obtaining higher density FE mesh in deepest regions**

***Cloud-based Supercomputer Implementation of PANC$^2$ Method***

Under a separate effort for a different client, Emc$^2$ is already implementing a cloud-based FE methodology on the Ohio Supercomputer Center for use by industry for simulating behavior of large welded structure (aerospace/transportation/energy/construction markets) prior to fabrication of these components. Given this extensive experience and that the open source software package WARP3D, extensively modified by Emc$^2$ staff already exists at Emc$^2$, the PANC$^2$ mesh generator and solution procedure will be implemented for commercialization of this technology for use by North American pipeline companies. TCPL has already indicated their interest in use of such technology and will actively cooperate in the Phase 2 effort as a strategic partner and validate the methodology for commercialization beyond Phase 2.

***Laboratory and Full-Scale Experiments on Pipe and Fittings***

During Phase 1 of this effort, preliminary laboratory tests on two grades of pipe (one old and one new) were conducted to prove the feasibility and the need for a new and more accurate prediction of the remaining strength of corroded pipes and fittings. During the Phase 2 effort, in addition to more laboratory experiments (tensile, strap tensile and SENT), a matrix of full-scale hydrostatic tests on corroded pipe shall be conducted. Per discussions amongst the project team members and the COR during Phase 1, it is anticipated that a 'grit blasting' method will be used to create artificial irregular-shaped corrosion-type defects on the outer surface of pipes and fittings and then these samples will be tested to failure hydrostatically to confirm the analytical predictions of the PANC$^2$ approach. The specific matrix for both the coupon and the full-scale experiments will be detailed in the Phase 2 proposal for this effort which may include combined loading (pressure + bending), geometric irregular-shaped discontinuities, as well as flaw interactions and separation distance will be investigated to predict the failure behavior and remaining strength more accurately.

***Implementation of Validated Failure Criteria into PANC$^2$***

Based on the Phase 1 effort new failure criteria that accurately account for both the grade (strength) of the pipe as well as the level of notch acuity will be implemented into the FE prediction methodology. These criteria will also enable accurate prediction of the effects of combined loading on corrosion type defects and the effects of the interaction of adjacent flaws on remaining failure strength. Based on the additional laboratory and full-scale experiments, any modifications to these criteria need to be developed. Specifically, if more sophisticated damage mechanics models based on accumulated plastic strain for various grades of pipe materials are needed they will be implemented into the PANC$^2$ method after being validated using the experimental data described above.

## ***References***


[1] B31G-2012, "Manual for Determining the Remaining Strength of Corroded Pipelines".

[2] G. Wilkowski, D. Rudland, P. Mincer, and D. Rider, and W. Sloterdijk "When Old Line Pipe Initiates Fractures in a Ductile Manner," paper # IPC2006-10326, *2006 International Pipeline Conference*, September 25-29, 2006.

[3] Kanninen, M. F., Zahoor, A., Wilkowski, G., Abou-Sayed, I., Marschall, C., Broek, D., Sampath, S., Rhee, H., and Ahmad, J., "Instability Predictions for Circumferentially Cracked Type 304 Stainless Steel Pipes Under Dynamic Loadings," EPRI Report NP-2347, April 1982.

[4] S. Rahman and G. Wilkowski, "Net-section-collapse analysis of circumferentially cracked Cylinder - part I: arbitrary-shaped cracks and generalized equations," *Engineering Fracture Mechanics*, 61 (1998), pp. 191 to 211.

[5] DET NORSKE VERITAS, *Recommended Practice DNV-RP-F108*, "Fracture Control for Pipeline Installation Methods Introducing Cyclic Plastic Strain," January 2006.

[6] G. M. Wilkowski and W. A. Maxey, "Applications of the Electric Potential Method for Measuring Crack Growth in Specimens, Flawed Pipes, and Pressure Vessels," *ASTM 14th National Symposium on Fracture Mechanics*, Los Angeles, California, ASTM STP 791, June 30, 1981.

[7] G. M. Wilkowski, J.O. Wambaugh and K. Prabhat, "Single Specimen J-Resistance Curve Evaluations Using the Direct-Current Electric Potential Method and a Computerized Data Acquisition System," *ASTM 15th National Symposium on Fracture Mechanics*, ASTM STP 833, June, 1982, pp. 553-576.

[8] G. Wilkowski, D-J. Shim, Y. Hioe, S. Kalyanam, and F. Brust, "How New Vintage Line-Pipe Steel Fracture Properties Differ from Old Vintage Line-Pipe Steels," paper IPC2012-90518, *Proceedings of the 9th International Pipeline Conference - IPC2012*, September 24 – September 28, 2012.

[9] D.-J. Shim, G. Wilkowski, D. Rudland, B. Rothwell, and J. Merritt, "Numerical Simulation Of Dynamic Ductile Fracture Propagation Using Cohesive Zone Modeling," paper # IPC2008-64049, *Proceedings of IPC2008 7th International Pipeline Conference*.

[10] Kiefner, J.F., Maxey, W.A., and Eiber, W. A., "A Study of the Causes of Failures of Defects that Have Survived a Prior Hydrostatic Test," NG-18 Report 111, May 1978.

[11] B31G-2012, "Manual for Determining the Remaining Strength of Corroded Pipelines".

[12] https://www.osc.edu/supercomputing/computing/ruby

[13] http://kiefner.com/wp-content/uploads/2013/05/KAPA.pdf

# Appendix A
# State of the Art in 2015 for Calculating the Remaining Strength of Corroded Pipe

By

John F. Kiefner

## Contents

Development of the B31G/RSTRENG and Other Models ..... 2
B31G ..... 2
Modified B31G and RSTRENG ..... 2
Models Other than B31G/RSTRENG ..... 3
Comparisons of the Models to Burst Test Results (the "Advantica" study) ..... 3
The Effects of High Strength on the Performance of Corrosion Assessment Models ..... 4
GL Phase 1 Work: Assessment of Corrosion in Higher Strength Pipe ..... 5
GL Phase 2 Work: Assessment of Corrosion in Higher Strength Pipe ..... 7
Tensile Tests ..... 7
Burst Tests ..... 9
Analysis of Corroded Pipelines Subjected to Internal Pressure and Secondary Loads ..... 10
Recent Work Sponsored by PRCI on the Assessment of High Strength Pipe affected by Corrosion ..... 11
Background ..... 11
Discussion of Task 1 ..... 12
Discussion of Task II ..... 13
Discussion of Task III ..... 14
Discussion of Task IV ..... 15
Discussion of Task V ..... 18
Discussion of Task VI ..... 21
Summary of the Key Findings of Project EC2-5 ..... 23
Summary of Findings on B31G/Mod B31G/RSTRENG ..... 24

# Development of the B31G/RSTRENG and Other Models

## B31G

The need for a valid model to assess the remaining strength of corroded pipe became sufficiently urgent in the late 1960s that the pipeline industry through the American Gas Association (AGA) sponsored an effort at Battelle to study the bursting behavior of corroded pipe. Forty-seven full scale burst tests were conducted on samples of pipe containing actual corrosion-caused metal loss, and a variation of Maxey's surface flaw equation[i] that embodied the "Folias factor"[ii] to account for bulging of the corrosion-weakened pipe and "flow stress"[iii] to account for the failure strength of the pipe material was found to give reasonable predictions of the failure stresses[iv].

The advent of in-line inspection (ILI) tools in the 1970s that could locate and characterize the sizes of areas of corrosion-caused metal loss in a buried pipeline encouraged the industry to standardize a method for calculating the remaining strength of corroded pipe based on the dimensions of the metal missing. The model developed previously at Battelle for AGA was embodied in a new standard in 1984: ASME B31G[v].

## Modified B31G and RSTRENG

While the B31G model served the purpose for ranking ILI anomalies, its highly simplified and over-conservative treatment of long corrosion on the basis of minimum remaining thickness resulted in large numbers of unneeded excavations. Therefore, AGA once again funded a project at Battelle in 1988 that involved developing a less conservative approach to predicting the remaining strength of corroded pipe. This project[vi] resulted in the development of the Modified B31G model that considers the axial length and depth of the anomaly with no limit on length and an iterative model named RSTRENG that considers the detailed depths of the corrosion within an "effective" length. Additional burst test data acquired mostly from pipeline operators' in-house tests of corroded pipe were added to the database[vii] bringing the total number of tests in the database to 124 not all of which were suitable for analysis by the B31G/RSTRENG approaches (e.g., tests involving brittle fracture initiation, defects aligned in the transverse or diagonal directions, multiple interacting defects, etc. were not used in the evaluation of the models). At this point the B31G-Modified B31G-RSTRENG suite of models had been validated by 86 full scale burst tests.

The Pipeline Research Council International (PRCI) funded additional work in the mid-1990s at Kiefner and Associates, Inc., the objective of which was to enhance the database of corroded pipe tests by including newly acquired data from burst tests on pipes with machined defects[viii]. The total number of burst test results in the database had grown to 216 by this time, 168 of which were suitable for assessing the accuracy of the predictive models. However, the highest grade of material in the database at this time was X65. No data were available to assess the applicability of the B31G/RSTRENG models to higher grades of pipe such as X80 and X100.

In 2009 ASME B31G was revised to include the Modified B31G equation and provisions for more sophisticated analysis of metal loss effects including a description of the "effective area" approach. RSTRENG is an example of an effective area approach. The latest ASME B31G document is a slightly revised version issued in 2012[ix].

## Models Other than B31G/RSTRENG

In the meantime other models for assessing the remaining strength of corroded pipe had evolved and were being used by some pipeline operators in place of or in addition to the B31G/RSTRENG models. One of these, LPC-1[x] was embodied in the standard DNV RP-F101[xi]. A second, called PCORR[xii] was developed at Battelle, and the third was called SHELL92[xiii]. The latter is identical to the Level 1[1] assessment model for locally-thinned areas embodied in API RP 579[xiv]. Along with the development of these models, additional burst test data were acquired. In many cases the additional data were generated by testing pipes containing corrosion-simulating machined defects.

## Comparisons of the Models to Burst Test Results (the "Advantica" study)

In 2005, the U.S. Department of Transportation (DOT) funded a project with GL Industrial Services UK Ltd (known as Advantica at the outset of the project) to evaluate ASME B31G, Modified B31G, RSTRENG, LPC-1, SHELL92, and PCORR and compare them to the burst test results in the AGA/PRCI database and the additional burst test results acquired in conjunction with the development of the newer models. The results of these evaluations were presented in Reference XV (the Advantica study)[xv]. Failure pressures predicted by each of the six models (denoted as $P_f$) were compared to actual failure pressures determined in the burst tests (denoted as $P_A$). The degree of scatter and the bias of the parameter, $P_A/P_f$, were used to assess the accuracy and inherent conservatism of each model. A database of 313 burst tests was compiled consisting of data from tests conducted by AGA/PRCI, GL, Petrobras, the Korean Gas Corporation, the University of Waterloo, and a couple of pipeline operators. Of these 313 results, 133 were obtained through tests of actually corroded pipe, and 180 were obtained through tests of pipe or ring specimens containing machined corrosion-simulating defects. In the case of the pipe specimens, the machined defects had uniform depths and various lengths. In the cases of most of the ring specimens, the machined defects had uniform depths clear across the width of each ring.

The $P_A/P_f$ comparisons for each of the six models were done in six ways called "cases". Case 1 comparisons involved using actual wall thicknesses and material properties and the definitions of flow stress normally associated with each model. Case 1 comparisons served as the measurement of the accuracy of each model. Case 2 comparisons were intended to show model performance in terms of reliably predicting a given factor of safety when used as a means of ranking ILI-detected anomalies. In Case 2 comparisons, nominal wall thickness and specified minimum material properties and the definitions of flow stress for each model were used. Cases 3-6 involved calculations based on various definitions of flow stress and are not as useful for assessing the performance of the models as the Case 1 and Case 2 comparisons.

The Advantica study provides many details on the performance of the six models making it the most thorough compilation of comparisons to date. While it is impractical to discuss all of them

---

[1] Level 1 models are sometimes called 2-parameter models because they consider only the overall length and maximum depth of an anomaly whereas other models such as RSTRENG and the more sophisticated computer models from which LPC-1 and PCORRC are derived are capable of considering the details of depth along the length of an anomaly. The Level 1 models are essential for analyzing most ILI data because the anomaly listings from the ILI vendor often present only the length, depth, and width of the anomalies.

in this review document, the essence of the findings can be summarized as follows. In terms of scatter the following table shows the frequency distributions of the ratios of actual failure pressures to model-predicted failure pressures for the six models on the basis of the 313 tests. For Case 1 analyses, RSTRENG predictions exhibit the least scatter.

Table 1 Comparisons of corrosion assessment models on the basis of burst test statistics

| Model | $P_A/P_f$ Distribution | |
|---|---|---|
| | Mean | Standard Deviation |
| ASME B31G | 1.330 | 0.468 |
| Modified ASME B31G | 1.184 | 0.285 |
| RSTRENG | 1.170 | 0.177 |
| LPC-1 | 1.178 | 0.318 |
| PCORRC | 1.191 | 0.310 |
| SHELL92 | 1.436 | 0.407 |

The Original ASME B31G model performed least well in terms of scatter, but Modified ASME B31G exhibited less scatter than four other Level 1 models.

Models such as B31G and Modified B31G are inappropriate for predicting failure pressures for uniform-depth defects, but as the Case 2 comparisons show, they provide conservative predictions of safe operating pressures when applied with a safety factor of 1.25 or 1.39 to real corrosion defects in materials with specified minimum yield strengths of 70,000 psi or less.

The authors of the Advantica study suggest that further evaluations of the models should be made by conducting burst tests on higher-grade materials (i.e., X80 and X100) using defects that are designed to simulate actual corrosion-caused metal loss rather than uniform-depth machined defects.

## The Effects of High Strength on the Performance of Corrosion Assessment Models

With the increasing use of high-strength line pipe (e.g., grades X80 and X100), concern has arisen over possible inadequacies of the current corrosion assessment models (i.e., B31G, Modified B31G, RSTRENG) for analysis of corrosion-caused metal loss in higher grades of line pipe materials. These materials, particularly X100 materials, tend to have yield-strength/tensile-strength (Y/T) ratios in the range 0.93-0.97, low strain-hardening capacity and low strain to failure. The high Y/T ratios make the use of the common definitions of flow stress (1.1SMYS for B31G, SMYS + 10,000 psi for Modified B31G and RSTRENG) questionable. Also, the effect of low-strain to failure is thought to be a factor that could affect the applicability of the models.

## GL Phase 1 Work: Assessment of Corrosion in Higher Strength Pipe

GL Industrial Services undertook additional work funded jointly be DOT and PRCI known as Project #153H aimed at reviewing the effectiveness of current corrosion assessment models for evaluating corrosion-caused metal loss in higher-strength line-pipe materials[xvi]. This report was published in August of 2009. The objectives of Phase 1 of this work were to review existing - burst-test data on higher strength materials to see how well the current models had predicted the actual failure pressures and to see how well a finite-element (FE) model would predict the actual failure pressures.

The finite element (FE) models used in this study are said to be described in Appendix G of BS7910[xvii]. Non-linear, large deformation stress analyses were performed using appropriate software packages. The vessel tests were analyzed using a 3D model, and the ring tests were modeled using a 2D model. Three stages of loading were used; linear-elastic behavior up to the onset of yielding, yielding spreading through the remaining ligament of the defect, and increasing stress with strain hardening until the von Mises equivalent stress reached the ultimate tensile stress, the latter point being used to define the failure pressure. The failure pressures predicted in this manner were compared to the actual failure pressures of X100 pipe materials (four tests altogether) containing machined, uniform-depth axial grooves or patches and to failure pressures of 10 ring specimens from the X100 pipe materials. The results of the comparisons are described below in conjunction with the comparisons obtained using the current models (i.e., B31G, Modified B31G, RSTRENG, and LPC-1).

Within the database of corroded pipe burst tests reviewed in Reference XV were eight burst tests of X80 pipe samples, four burst tests of X100 pipe samples, and 37 ring tests. In Phase 1 the actual failure pressures obtained in these tests were compared to the failure pressures predicted by the current models and by the FE analysis.

Four of the eight X80 burst tests were conducted on a material with a diameter-to-thickness (D/t) ratio of 62 and a Y/T ratio of 0.81. The other four X80 burst tests were conducted on a material with a D/t ratio of 82 and a Y/T ratio of 0.80. The Y/T ratios of both of these materials do not seem to represent a low-strain-hardening capability, nor does it seem likely that the definitions of flow stress as 1.1 the actual yield strength or the actual yield strength + 10,000 psi would cause inaccurate predictions. In fact the B31G comparisons were made on the basis of flow stress being defined as 1.1 times the actual yield strength, and the MOD B31G and RSTRENG comparisons were made on the basis of flow stress being defined as the actual yield strength plus 10,000 psi. Machined, uniform-depth, axial grooves were used to simulate corrosion-caused metal loss. The lengths of the defects in the tests were either 3.9 or 4.5 times $\sqrt{Dt}$ meaning that they were "long" defects. Defect depth/thickness ratios ranged from 0.089 to 0.782. The ratios of actual failure pressures, $P_A$, to predicted failure pressures, $P_f$, were as follows.

Table 2 Ranges of ratios of actual to predicted failure pressures from tests done as part of the GL Phase 1 work – 8 samples of X80 pipe

| | B31G | MOD B31G | RSTRENG | LPC-1 |
|---|---|---|---|---|
| MAX | 1.443* | 1.195 | 1.232 | 1.176 |
| MIN | 0.67** | 0.745** | 1.099 | 0.993 |
| RANGE | 0.773 | 0.45 | 0.133 | 0.183 |
| AVG | 1.160625 | 1.057 | 1.179625 | 1.1155 |

*B31G defaulted to the remaining thickness and infinite length for the $4.5\sqrt{Dt}$ cases.
**These low values result because these models consider metal loss areas that are less than the actual areas.

The results indicate that RSTRENG was able to predict the failure pressures with reasonable accuracy using the yield strength + 10,000 psi as the flow stress. The predictions based on B31G and MOD B31G show what was already known, namely, that these methods are unsuitable for uniform-depth defects.

Four burst tests of an X100 material with D/t of 58, Y/T of 0.98, two with patch defects and two with axial groove defects were carried out. Machined, uniform-depth, axial grooves or patches were used to simulate corrosion-caused metal loss. The lengths of the defects ranged from $3\sqrt{Dt}$ to $6.3\sqrt{Dt}$. Depths were about 50% of the wall thickness in all four samples. In view of the very high Y/T ratio, one might question whether the normal definitions of flow stress would be adequate. Nevertheless, the B31G comparisons were made on the basis of flow stress being defined as 1.1 times the actual yield strength, and the MOD B31G and RSTRENG comparisons were made on the basis of flow stress being defined as the actual yield strength plus 10,000 psi. The ratios of actual failure pressures, $P_A$, to predicted failure pressures, $P_f$, were as follows. Note that the comparisons for FE analysis are included.

Table 3 Ranges of ratios of actual to predicted failure pressures from tests done as part of the GL Phase 1 work – 4 samples of X100 pipe

| | B31G | MOD B31G | RSTRENG | LPC-1 | Finite Element |
|---|---|---|---|---|---|
| MAX | 1.175* | 1.021 | 1.136 | 1.045 | 1.299 |
| MIN | 0.909** | 0.897** | 1.012 | 0.96 | 1.027 |
| RANGE | 0.266 | 0.124 | 0.124 | 0.085 | 0.272 |
| AVG | 1.04 | 0.95925 | 1.074 | 1.00125 | 1.11525 |

*B31G defaulted to the remaining thickness and infinite length for the cases where the lengths exceeded $4\sqrt{Dt}$.
**These low values result because these models consider metal loss areas that are less than the actual areas.

The results indicate that RSTRENG was able to predict the failure pressures with reasonable accuracy using the yield strength plus 10,000 psi as the flow stress. The non-linear FE method gave failure predictions exhibiting more scatter than RSTRENG did.

RSTRENG predictions for 28 of the 37 ring tests gave the following comparisons ($P_A/P_f$) with actual failure pressures (9 of the comparisons were judged invalid by the GL team):

MAX = 1.237 MIN = 0.931 RANGE = 0.306 AVG = 1.167 STDEV = 0.061

It is recalled that RSTRENG has been validated primarily on the results of tests of end-capped pipe samples (i.e., pressure vessels). It is likely that yielding would occur in a ring test at a lower pressure level than that associated with the yielding of the same material in the form of an end-capped pressure vessel. This is because the axial stress in the pressure vessel causes the effective yield stress to be higher than that in a uniaxially-stressed ring specimen. This effect could result in lower failure pressures in ring specimens. Nevertheless, the average ratio of RSTRENG-predicted failure pressures to ring test failure pressure is greater than one. The lowest prediction ratio was associated with a test involving a notch-like groove that may not have represented corrosion-caused metal loss very well.

The authors of Reference XVI concluded that RSTRENG adequately predicts the failure pressures for corrosion-like defects in higher strength materials such as X80 and X100 even when flow stress is defined as the yield strength plus 10,000 psi. However, they show that more conservative results would result from using the average of yield and ultimate strength as the flow stress. They implied that B31G and Modified B31G may also be adequate for higher strength materials, but that cannot be proven one way or another by means of tests on uniform-depth defects. They suggest conducting tests on higher strength materials with defects created by corrosion-like metal removal methods that would result in defects that look more like actual corrosion defects.

## GL Phase 2 Work: Assessment of Corrosion in Higher Strength Pipe

The report on the second phase of Project #153H[xviii] was published in November of 2009. The objectives of the Phase 2 effort were to examine the degree of variation in tensile properties of X100 line pipe across the wall thickness, to examine the differences in tensile properties in the axial and circumferential directions, to conduct two additional burst tests on samples of X100 pipe containing metal loss defects, and to construct failure loci for metal loss in X100 pipe subjected to both circumferential loading (i.e., pressure-induced hoop stress) and externally applied axial loads. In this report it was revealed that parallel efforts were underway at GL as part of Project #153 to evaluate the effects of bi-axial stress, cyclic pressure loading, low toughness, and the interaction of closely spaced defects on the ability to accurately predict failure pressures of corroded pipe using the B31G/RSTRENG suite of assessment methods. It was further revealed that GL was assisting BP in a proprietary operational trial of X100 pipe that included looking at the effects of metal loss on the performance of the pipe. These results of these parallel efforts are reported in separate reports.

### Tensile Tests

Tensile tests were conducted on samples removed from X100 DSAW pipes made by three different manufacturers. Two of the pipes were 48-inch-OD (Manufacturers A and B), and one was 52-inch-OD (Manufacturer C). The main objective of these tests was to be able to analyze the effects of biaxial loading on the yielding behavior of X100 materials anticipating that these pipe materials are likely to exhibit non-isotropic yielding behavior. The manufacturers' tests data are shown in the following table.

Table 3 Results of manufacturers' tensile tests on three X100 materials involved in the GL Phase II work

| Manufacturer | | Transverse | | | Longitudinal | | |
|---|---|---|---|---|---|---|---|
| | | Yield Strength, psi | Tensile Strength, psi | Y/T | Yield Strength, psi | Tensile Strength, psi | Y/T |
| A | Average of three specimens | 121,487 | 130,624 | 0.93 | 97,170 | 126,369 | 0.77 |
| B | Average of two specimens | 108,410 | 120,302 | 0.90 | 93,762 | 116,749 | 0.80 |
| C | Average of three specimens | 106,114 | 114,235 | 0.93 | 96,493 | 111,141 | 0.87 |

Based on the manufacturers' tests all specimens tested in the transverse (circumferential) direction exhibited yield and tensile strengths that exceeded the minimum requirements of API Specification 5L, 44th edition, for X100 pipe, and the Y/T ratios were 0.93 or less. The yield and tensile strengths measured in the longitudinal tests were all lower than those measured in transverse tests. Most likely the specimens for these tests were flattened strap-tensile specimens.

GL's tensile tests consisted of numerous miniature flat tensile (MFT) tests, standard round-bar tensile (ST) tests, and two ring tension tests on each of the three samples of X100 material. The MFT specimens had a thickness of 0.5 mm and a width of 2 mm in the gage section, and ten specimens were obtained through the wall thickness. The intent was to gain insight into the variations in strength through the wall thickness that could be anticipated from the pipe forming process (U-ing and O-ing). Both transverse and longitudinal specimens were created to examine the differences in yielding behavior in those directions. Lastly, samples for the MFT and ST tests were taken from both the 3 o'clock and 6 o'clock positions with respect to the seam weld to examine variations around the circumference of the pipe.

Because of their small size, the MFT specimens had to be created by electro-discharge machining and tested at a special facility. The discussion of the results of these tests suggests that they gave only relative results. Absolute MFT results were inferred by extrapolation from the ST results. The behaviors of the MFT specimens seemed erratic to this reviewer, and might lead one to question their value. According to the authors, "There was no identifiable pattern of tensile property variation through the wall thickness." The authors suggested that the MFT specimens probably should have been made twice as thick as they were and that only five specimens should have been created at each location.

The authors state that, "From the standard tensile (ST) test results, it was concluded that tensile properties in the longitudinal direction tended to be lower than those in the transverse direction", but not in every case when individual test results are reviewed. When one looks at the stress-strain curves, it looks like there may have been a mix-up in the labeling of the specimens in the two cases where the longitudinal yield strengths appear to have exceeded the transverse yield strengths. The shapes of the curves suggest as much. It would be useful to

have the authors consider the possibility that the symbols for transverse and longitudinal may have been accidentally interchanged.

The two ring tensile test samples from the pipes produced by Manufacturers A and B failed after the beginning of yielding but prior to the attainment of 0.5% total elongation as required for a measurement of yield strength. All four of these rings failed at the toe of the DSAW seam. These failures occurred at hoop stress levels above 120,000 psi, so the yield strengths of the base metals in these two pipes exceeded the expected minimum level of 100,000 psi. A total elongation of more than 0.5% was attained in each of the two ring tensile tests of the pipe produced by Manufacturer C. The yield strengths exceeded 106,000 psi.

## Burst Tests

Two burst tests were conducted on samples of the 52-inch-OD, 0.812-inch-wall X100 pipe supplied by Manufacturer C. The samples contained longitudinally-oriented grooves simulating corrosion-caused metal loss. Both grooves were machined by means of a spherically-shaped tool to a depth of 50% of the wall thickness. The radius of each groove was 0.5 times the wall thickness. The groove in the Test 1 was 79 inches long, and the groove in Test 2 was 29 inches long. The pipes were fabricated with extension pups and end caps and pressurized to failure with water as the test medium. Test 1 ruptured at 1,755 psig; Test 2 ruptured at 1,987 psig. Both ruptures initiated at the machined grooves.

The authors compared these burst pressures to the predictions of failure pressures of the various models, stating the following results in terms of $P_A/P_f$ ratios. Specified minimum tensile properties were used in each case.

| Test Number | ASME B31G | Mod ASME B31G | RSTRENG | LPC-1 | SHELL92 |
|---|---|---|---|---|---|
| 1 | 1.08 | 0.88 | 0.97 | 1.00 | 1.03 |
| 2 | 1.15 | 0.88 | 0.97 | 0.94 | 1.01 |

Similar, though not identical, $P_A/P_f$ values were obtained by this reviewer using KAPA (software that usually gives calculated failure pressures identical to those obtained via RSTRENG).

- ASME B31G: 1755/1718 = 1.02 for Test 1, 1987/2493 = 0.80 for Test 2.
- Modified B31G: 1755/2086 = 0.84 for Test 1, 1987/2250 = 0.88 for Test 2.
- KAPA: 1755/1834 = 0.96 for Test 1, 1987/2015 = 0.99 for Test 2.

Note that the 29-inch flaw of Test 2 is at the boundary limit of $\sqrt{20Dt}$ where the B31G equation changes to considering the flaw to be parabolic in shape to a flaw with constant depth over an infinite length. For a flaw of 29-inches or less, the parabolic flaw shape is assumed. If one uses the infinite length version, the $P_A/P_f$ ratio for Test 2 via B31G is 1987/1718 = 1.16. The flow stress used in KAPA was taken to be SMYS + 10,000 psi, in other words, 110,000 psi. This would put it very close to the average of the yield and ultimate strengths of the material as measured in the manufacturer's transverse yield and tensile strength tests: 106,114 psi and 114,235 psi, respectively, for an average of 110,174 psi.

The authors acknowledge that Modified B31G cannot be expected to give accurate predictions for uniform-depth flaws because it only considers 85% of the area of the rectangular shape of a uniform-depth flaw of finite length. The authors seem to be implying that the $P_A/P_f$ ratios of near 1.0 given by RESTRENG means that RSTRENG can be used for predicting failure pressures for uniform-depth, blunt flaws in an X100 material.

## Analysis of Corroded Pipelines Subjected to Internal Pressure and Secondary Loads

The analysis of the strength of corroded pipe under combined loadings was described in a previous study conducted by GL[xix]. In that study, finite element analysis was employed to assess the effects of combined internal pressure and external loading on the failure of corrosion defects in materials of Grades X42 and X65. As stated previously, part of the report being reviewed here was dedicated to extending the analysis to X80 and X100 materials. The stress-strain curves generated by means of the tensile tests described previously were used to facilitate the non-linear, elastic-plastic finite element analysis of corroded pipes under combined stress conditions.

Three-dimensional non-linear finite element models were created to simulate rectangular "patches" of corrosion, axially-oriented grooves, circumferentially-oriented grooves, and isolated spherical pits having depths of 20%, 50%, and 80% of the wall thickness. A "local" failure was deemed to occur when the remaining ligament either "necks" or buckles in response to a given combination of internal pressure and external load. A "global failure was deemed to occur when the von Mises equivalent stress reaches the yield strength of the material. Normalized failure loci diagrams were created for either ratios of applied compressive axial force divided by "critical" compressive axial force or ratios of applied moment divided by "critical" moment versus ratios of applied pressure divided by "critical" pressure of each type-of-defect/defect-depth combination.

The authors recommended that "the normalized failure loci diagrams derived in this report should be incorporated into the PRCI Guidance Document[xx] for assessing corrosion damage in pipelines." The failure loci likely will be used only in special circumstances where a pipeline is subjected to unusual external loads. For most applications criteria such as B31G, Modified B31G, or RSTRENG would be sufficient to assess the remaining strength of corroded pipe. The following quote from Reference XIX helps to put the failure loci in perspective:

> *"These methods (i.e., B31G, Modified B31G, RSTRENG) were derived based on experimental tests and theoretical/numerical studies of the failure behavior of corroded pipelines subjected only to internal pressure loading. In the vast majority of cases, internal pressure loading will be the main loading mechanism on the pipeline. However, there may be instances when pipelines could also be subjected to significant loading from the environment. For onshore pipelines, these additional loads could be as a result of ground movement due to landslides, mining subsidence, or even seismic activity. In the case of offshore pipelines the formation of free spans may impose significant bending loads. For instance, seabed scour can lead to the development and growth of free spans of pipelines resting on the seabed, particularly if they are not trenched. Whilst, the guidance detailed in standard assessment methods will be sufficient in the majority of cases, it may be inappropriate or non-conservative to use it in cases when the pipeline may also be subjected to significant external loading. The objective of this project is to extend existing methods to allow assessment of corroded pipelines that are subject to*

*both internal pressure and external loading. Development of this new guidance will remove an important area of uncertainty in the assessment methods currently used by the pipeline industry."*

## Recent Work Sponsored by PRCI on the Assessment of High Strength Pipe affected by Corrosion

### Background

PRCI Project EC2-5 was conducted at Battelle[xxi] for the purposes of consolidating data from full-scale burst tests of corroded pipe and using the data to determine whether or not the commonly-used metal-loss assessment equations are consistent across all grades of line pipe from Grade A through Grade X100. The authors refer to high-strength grades of steel as line pipe steels of Grade X70 and up and refer to them by the acronym "HSS" steels or "HSS" pipe. All other materials are referred to as "vintage" materials. The term "vintage" is overly broad if meant to be applied to all materials of Grades below X70. Newer steels of Grades X52, X60, and X65 tend to exhibit strain-hardening characteristics that may be quite different from those exhibited by older materials of the same grade and have different microstructure, chemistry and lower inclusion content. It cannot be assumed that these newer materials will behave the same as the older materials of the same grade in response to limit loads associated with failures from excessive metal loss. Hence, some scoping tests may be necessary to establish whether or not the B31G models are applicable to these newer materials.

In this report a predictive model for failure stress of a corrosion defect is defined generically as the product of two factors, the first of which is the "reference stress". The reference stress is taken to mean the inherent resistance of the pipe to failure. In the B31G/RSTRENG suite of models, the reference stress is understood to be the flow stress of the material, and flow stress is defined either as 1.1SMYS or SMYS + 10,000 psi. For other models such as LPC-1 and PCORRC, the reference stress is generally assumed to be the ultimate tensile strength of the material.

The second factor represents the effects of pipe geometry and defect geometry. The B31G/Modified B31G models apply a "shape factor" to represent the complex geometry of the typical corrosion defect as a fixed portion of the rectangle formed by the overall length and maximum depth of the defect and a 'bulging factor" to account for the increase in stress in the remaining ligament of pipe resulting from weakening of the shell of the pipe. The shape and bulging effects are accounted for in the LPC-1 and PCORRC models implicitly by one factor determined through finite element analysis.

The authors note that the B31G/RSTRENG models were derived empirically through tests of corroded pipe and pipes containing blunt, corrosion-simulating flaws involving materials from Grade A through Grade X65. They also point out that the LPC-1 and PCORRC models were derived through finite element analyses and validated through test of corroded pipe materials of Grades X42 though X100.

The objectives of Project EC2-5 can be summarized as follows:

1. To assemble a database of tests of vintage pipe and HSS pipe by merging burst test results from the two classes of pipe materials.
2. To identify gaps in the database.
3. To determine whether or not the results of tests on machined flaws should be considered to adequately simulate the results of tests on real corrosion defects.
4. To use the database to show whether or not the various corroded-pipe assessment equations give adequate and consistent predictions of failure pressure over the entire database of results.
5. To modify the models as appropriate to assure adequate and consistent predictions.
6. To determine whether or not further full-scale testing was needed to resolve Objectives 2, 3, 4, and 5.

Project EC2-5 consisted of six technical tasks:

i. Gather burst test data on HSS pipe samples with metal loss. Two parts; small pits, high failure stress to examine reference stress trends, and large pits where geometry of the pipe and the defect control failure pressure.
ii. Expanding and restructuring the two parts of the database
iii. Assessing the role of testing practices
iv. Full-scale testing
v. Finite element analysis to assess reference stress for defect-free pipe, "river-bottom/shoulder effect", and flow properties in terms of Y/T.
vi. Assess the corrosion-assessment criteria in terms of margin of safety and grade of pipe. Look for gaps and a means to bridge them.

## Discussion of Task 1

In pursuit of Task I, the authors compiled a database of tests on corroded samples and samples containing corrosion-simulating defects that spanned materials from Grade A through Grade X100. They sought test results on samples with large ranges of materials and large ranges of flaw sizes. They suggest that results involving small flaws (sizes trending to zero) would be of help in identifying the unifying definition of reference stress whereas results involving large flaws would tend to be more useful in examining the effects of bulging and shape factors.

Most of the Battelle team's database consists of the "GL R6781 Database" from the "Advantica" study (Reference XV in this reviewer's list). The GL R6781 database contains 313 burst test results, 49 of which were obtained through tests of high-strength steels containing machined, uniform depth flaws. The GL R6871 database is presented in Table A1 in "Annex A" of Battelle's report, and it is identical to the data listed in the Advantica study, Reference XV. It appears the column headings in Battelle's Table A1 labeled "d/t" and "$L/\sqrt{Dt}$" have been interchanged. Assuming that to be the case, it is hard to understand the meaning of the very large $L/\sqrt{Dt}$ values listed for Test Numbers ranging from 135 to 146, 248 to 254, and 263-299. It turns out that these tests are ring-expansion tests whereas the remainder of the tests involved burst tests of end-capped pressure vessels. The L/√Dt values for ring tests should be very low values, because L is ~3 inches in every case.

Index Numbers 248-254 involved 7 ring-expansion tests of an X60 material, and thus are not considered HSS materials via Battelle's definition. Index Numbers 255-262 involved 8 pressure-vessel tests of two X80 materials (four tests each). Index Numbers 263-299 involved 37 ring-expansion tests of two X100 materials, and Index Numbers 300-303 involved 4 pressure-vessel tests of an X100 material. The results of the 12 burst tests, 8 involving the X80 materials, and 4 involving the X100 material were discussed previously by this reviewer under the GL Phase I work, Reference XV.

The authors of the Battelle report discuss some "issues" with the database included missing data, missing parameters such as ultimate tensile strength, and the presentation of only D/t ratios as opposed to specific diameters and thicknesses. They also note that details of the testing scope and practices were limited. Apparently GL considered their database proprietary, but they released it "as is" to Battelle under a non-disclosure agreement. Later, many of the missing details were provided to the Battelle team so they could trend the data. The database with these details included is referred to as the GLND R6781 database and is presented in Table A2. Presumably the ND refers to non-disclosable. This database is labeled "confidential". Battelle is not permitted to distribute the database beyond the member companies of PRCI. <u>There is a gap in Table A2. Index Numbers 230 through 288 are missing.</u>

The Battelle team conducted an extensive literature search to find additional data, but the search yielded no satisfactory data to add to that contained in the GL R6781 database. However, they were able to gain access to the results of four full-scale burst tests of high-strength steel pipes containing simulated metal loss defects (referred to as the "Fluxys" tests) and a database of tests of defect-free high-strength steel pipes.

## Discussion of Task II

In Task II the Battelle team examined the results of the 49 HSS tests from the GLND R6781 database finding that 37 of them involved ring-expansion tests. They show that the ring-expansion results could have been predicted with a simple net-section-collapse (limit-load) analysis because defect length has no meaning in a ring-expansion test. They conclude that the ring-expansion tests are of no value to the overall effort of this project to validate a corroded-pipe analysis method the will be uniform across all grades of pipe. The authors of the Battelle report allude to the absence of a bulging effect because of the absence of the effects of pressure in a ring-expansion test. This depends on whether the ring-expansion test was performed by means of a mechanical expander or by means of actual fluid pressure. The original ring-expansion test was developed by Youngstown Sheet and Tube Company, and it was used by them almost exclusively to determine yield strength only. The tests were never intentionally continued to failure because a failure would damage the testing equipment. Youngstown's ring-expansion tests were carried out via pressurized liquid rather than a mechanical expansion device. If such a device was used by GL, then bulging at the defects could have been present. However, Battelle's decision to eliminate the 37 ring tests from their proposed database is sound. The ring tests offer no means to assess defect length or shape factor.

In the Battelle report the importance of "shape factor" is discussed by noting that Modified B31G (with its shape factor of 0.85) overestimated the results of four burst tests of an X100

material containing uniform-depth defects. It is further noted that if a shape factor of 1.0 instead of 0.85 is used, Modified B31G underestimates the results of the four burst tests.

The 12 pressure vessel tests involving HSS materials in the GL R6781 database, are presented in Table B3 of Appendix B of Battelle's report (Reference XXI). Eight of the 12 tests involved X80 materials, and 4 of the 12 tests involved X100 materials. These tests were discussed previously herein in the section on the GL Phase 1 work (see Tables 1 and 2). It is recalled that the failure pressures of the 12 tests were conservatively predicted via RSTRENG. It is noted that mistakes appear in Table B3. The values listed for d/t for the X80 materials (the first 8 tests) are the actual depths of the defects, not the d/t ratios. Moreover, the depths given in the d/t column for Tests 7 and 8 are incorrect. In the column labeled (Depth, inches) the values for the first 8 tests are incorrect.

The 12 Fluxys burst tests[2] were carried out on two X70 materials. The results are presented in Table B3 along with those of the 12 results from the HSS materials in the GL R6781 database and 3 tests described below under the discussion of Task IV. In the Fluxys test, four pressure vessels with three defects each were tested. Each of the defects in each vessel were of the same length and depth, but the widths varied from narrow slots to wide patches. In all four vessels, the widest defect failed, and other two did not fail. In effect this means that the Fluxys tests only produced 4 results that can be compared against failure pressure prediction models. So, the actual number of useable results in Table B3 is 19 rather than 27. RSTRENG predictions for the failures are presented later in this review.

The Battelle team suggests that these results show that width does affect the failure pressure contrary to what is normally assumed. It seems that wider defects tend to have lower failure pressures than narrower defects. This reviewer is inclined to agree, although the likely effect, for now at least, has only been documented in tests of uniform-depth machined defects. In fact, a review of the results of certain similar tests in Reference VIII (Index Numbers 119 through 124) showed a similar width effect though at the time it was attributed to unknown factors not related to width. The effect of width could be important, and further work on its effect is in order.

## Discussion of Task III

Task III of the Battelle study was aimed at examining the effects of test methods and of methods for creating defects on the credibility of the databases assembled under Tasks I and II. The choices of test methods would seem to include burst tests of pipe containing actual corrosion, burst tests of pipe containing artificially-made corrosion, and burst tests of pipe containing machined corrosion-simulating defects. Ring tests as discussed under the Task II work do not produce useful results for the database accumulated by Battelle. The absence of corroded HSS pipe necessitates using machined or artificial defects.

The report warns of tests of vessels containing multiple defects, where the effect of pressure cycles on tests of defects that have survived previous test cycles in which more-severe defects had failed can lead to pressure reversals. Indeed, this behavior was observed in some of the earliest testing of vintage corroded pipe at Battelle prior to the development of the B31G

[2] Fluxys is a Belgium gas company.

criterion. The Battelle team presents additional evidence of such behavior in vintage materials. This threat is said not to be significant with HSS materials based on the premise that the failure mode of plastic collapse is expected for HSS materials. This reviewer would argue that the reverse could be true. That is, the introduction of plastic strain at a near-failure defect in an HSS materials could result in a pressure reversal following the failure of an adjacent defect.

There is speculation in the Battelle report that the behavior of corroded pipe pulled from service is no different from that of pipe containing machined defects if plastic collapse is the failure mode. This is subsequently demonstrated by Battelle's Figure 4 based on the work of Bony, et. al (Battelle's Reference 26). Their Figure 4 shows that machined defects can legitimately be used as corrosion-simulating defects if the model used to predict failure pressure properly accounts for the shapes of the machined defects and actual metal loss.

The Battelle team uses as their Figure 5, a variation on a figure that was used in the "Continued Validation of RSTRENG", (their Reference 34 and Reference VIII herein) to define a "nested" defect, a shorter, deeper pit within a longer, shallower region of metal loss. Such defects can be easily machined and offer a better means than uniform-depth defects for assessing shape factors and the effects of ridges or shoulders that appear with real corrosion where pits overlap. The authors note that RSTRENG is capable of assessing such defects rather well for vintage materials and might do so for HSS materials if the correct reference stress is used. They also note, correctly, that RSTRENG is not capable of predicting whether a given corrosion anomaly will fail by leaking or by causing a rupture. This, they note, depends on pressure, toughness, and local defect geometry.

The section of the report on Task III is concluded with the thought that not enough burst test data have been generated with complex flaws especially for HSS materials. They recommend conducting further tests involving shorter features and nested features to strengthen the database and doing an analytical study to assess shape factors.

## Discussion of Task IV

Battelle's Task IV efforts on Project EC2-5 consisted of conducting three full-scale tests. The pipe material chosen for these tests was a 30-inch-OD, 0.625-inch-wall, X70M DSAW material with a Charpy V-notch plateau energy exceeding 200 ft-lb.

- Vessel One; a round feature 80% through the wall with a diameter of 4.5 inches and a rectangular feature with a length of 10 inches, a width of 6 inches, and a depth of 59% of the wall thickness.
- Vessel Two; a rectangular feature with a length of 6 inches, a width of 3 inches, and a depth of 80% of the wall thickness nested symmetrically within a rectangular feature with a length of 10 inches, a width of 6 inches, and a depth of 45% of the wall thickness.

A lot of thought went into planning the dimensions of the defects. The aim was to have the round feature in Vessel One fail as a leak at about the same pressure that the rectangular feature in the same pipe would fail as a rupture. The compound feature in Vessel Two was designed such that the nested defect would leak. A through-wall flaw failure equation developed on a previous PRCI project (EC2-3) referred to as TW-collapse was used to

accomplish this defect-length sizing. PCORRC, a Level 1 corrosion defect assessment model developed previously at Battelle for PRCI, was used to establish the desired surface flaw failure pressures. The three features were created by accelerated corrosion, so the final shapes were not necessarily equal to the target dimensions. However, measurements made after the defects had been fabricated showed that the final dimensions were not far off of the target dimensions. The actual dimensions are given in Appendix C of Battelle's report.

- The failure pressure of round feature in Vessel One was predicted via PCORRC on the basis of target dimensions to be 2,590 psig (88.8% of SMYS). The anticipated failure mode was a leak. This defect survived with significant bulging, a pressure level of 2,624 psig (90% of SMYS).
- The failure pressure of the uniform-depth rectangular feature in Vessel One on the basis of the target dimensions was predicted via PCORRC to be 2,601 psig (89.2% of SMYS). The anticipated failure mode was a rupture. The defect failed at a pressure level of 2,624 psig (90% of SMYS) and the failure occurred as a rupture that arrested near the ends of the defect.
- The failure pressure of the compound rectangular feature in Vessel Two on the basis of the target dimensions was predicted via PCORRC to be 2,136 psig (73.2% of SMYS). The anticipated failure mode was a leak within the nested portion. The defect failed at a pressure level of 2,036 psig (69.8% of SMYS), and the failure occurred as a leak near one end of the nested defect.

The results of 19 of the tests given in Battelle's Table B3 were used to validate the accuracy of PCORRC with regard to predicting failure pressures of corrosion anomalies in HSS pipe materials. The authors imply that PCORRC is more suited than other Level 1 assessment methods to account for the more extreme bulging associated with the failure of a corrosion anomaly in an HSS material. They also note that the one test with the compound (nested) defect demonstrates the "shoulder" effect.

RSTRENG predictions for the 19 tests on HSS materials are presented Figure 1, and PCORRC predictions for 18 of the 19 tests on HSS materials are presented in Figure 2.

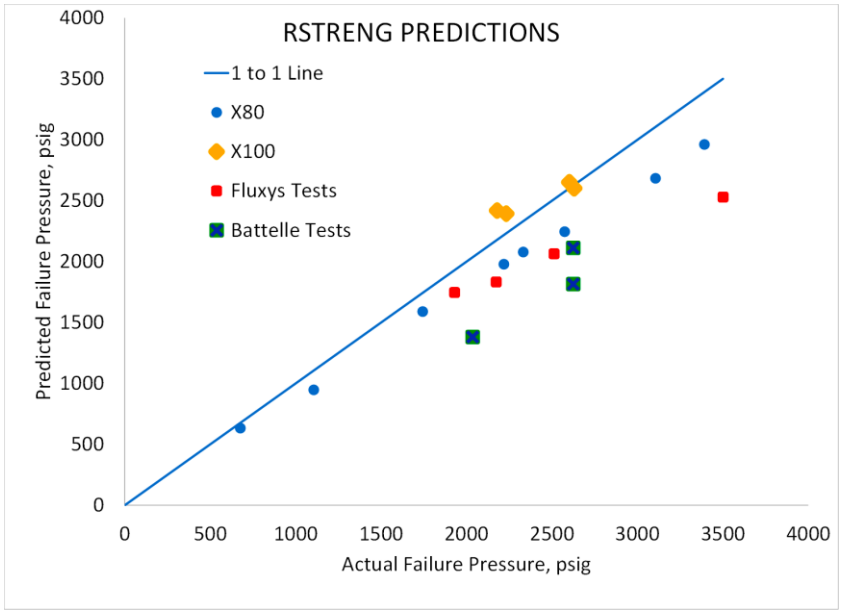


Figure 1 RSTRENG Predictions for the 19 HSS Burst Tests

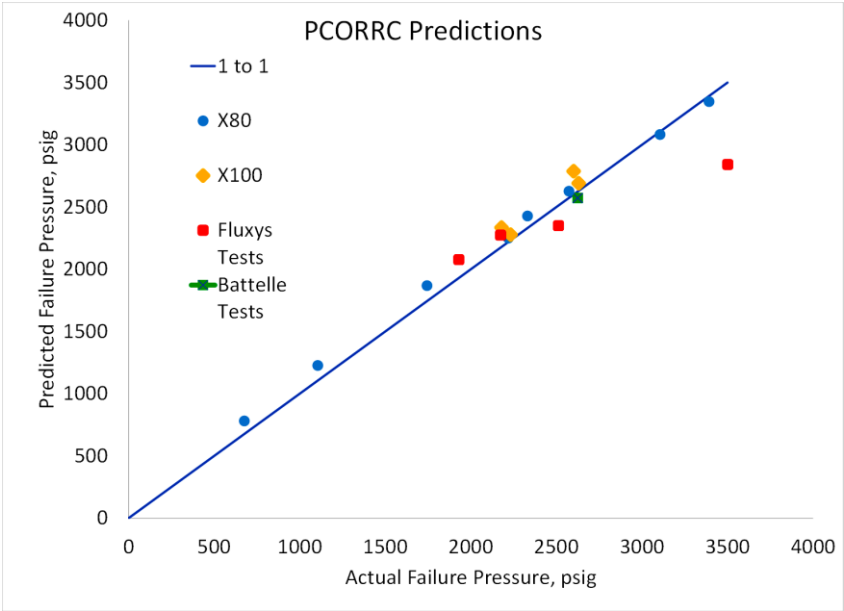


**Figure 2 PCORRC Predictions for 18 of the 19 HSS Burst Tests (PCORRC cannot handle the dimensions of the nested defect)**

The RSTRENG predictions are based on actual yield strength + 10,000 psi as the reference stress whereas PCORRC predictions are based on ultimate tensile strength as the reference stress. Both models gave reasonably accurate predictions.

The authors assert that the through-wall failure stress prediction model, TW-collapse, is useable to determine whether the failure of a given corrosion anomaly will be a leak or a rupture. The model did well in this role in the three full-scale tests performed by the Battelle team.

However, it would be appropriate to test the model against the large numbers of results of tests of actual corroded pipe in the GL R6781 database.

The authors note the complexity of trying to achieve a seamless approach to the assessment of corrosion anomalies across the entire range of HSS pipe materials and vintage pipe materials. They indicate that their Task V analysis is needed to understand how a seamless approach might be achieved.

## Discussion of Task V

One objective of Task V of Project EC2-5 was to assess the failure responses of different grades of pipe under plastic collapse conditions so that a single definition of reference stress could be applied to corrosion assessment models. As it stands currently, models such as RSTRENG/B31G utilize a reference stress based on SMYS because that was found to be appropriate for vintage materials. However, models such as PCORR/PCORRC and LPC-1 utilize a reference stress based on the ultimate tensile strength of the material. The latter has been found to be appropriate for HSS materials, and it would be desirable to utilize it across all grades of pipe.

The second objective of Task 5 was to assess the "shoulder" effect of ridges or depth discontinuities between overlapping pits to determine how these features affect bulging and the coalescence of pits that controls failure pressure and whether the resulting failure is a leak of a rupture.

In pursuit of the first objective, the Battelle team examined burst test data on defect-free pipe. They utilized three models of failure behavior, the von Mises criterion, the Tresca criterion, and their new "Z-L criterion" based on average shear stress to predict the burst pressures of defect-free pipes for a range of grades from Grade A to Grade X120. All three models consider strain-hardening effects. Because the actual strain-hardening behaviors of the materials in the database were not known in every case, they plotted the ratios of predicted to actual burst pressure varies versus the yield/tensile (Y/T) ratios on the premise that the Y/T ratio is a suitable substitute for the strain-hardening effect. The models tended to underpredict the failure pressures of the lower strength grades and overpredict the failure pressures of the higher strength grades. The authors point out that a reference stress definition that does not include strain hardening is subject to errors as large as 10%.

From vintage pipe materials, the authors show that flow stress defined as ultimate tensile strength (UTS) minus 20,000 psi gives about the same flow stress as that defined as SMYS plus 10,000 psi.

Next, they compared Modified B31G predictions of the failure pressures in the database of corroded pipe tests through 1989 using the reference stress defined as UTS - 20,000 psi to Modified B31G predictions using SMYS + 10,000 psi. The comparison showed an almost 1 to 1 relationship with only minor scatter (goodness of fit $R^2 = 0.93$). This, they suggest, means that Modified B31G could be used with a flow stress defined in terms of UTS rather than SMYS and that a generalized reference stress for all grades of pipe based on UTS could be realized. Because UTS is generally not known, they also explored using specified minimum ultimate strength (SMTS) to define the reference stress. Again using Modified B31G, the authors found a good correlation between predictions using SMYS + 10,000 psi as flow stress and those using

SMTS – 10,800 psi as flow stress. They assert that using the SMTS relationship in the RSTRENG/B31G family of models for predicting failure pressures of corrosion anomalies in vintage materials could be a way of achieving a seamless reference stress definition over the range of materials from Grade A through Grade X120.

The Battelle team then compared the actual failure stress levels of defect-free pipes to UTS, SMTS, and SMYS. These comparisons were said to show that UTS is the best predictor of full-scale burst test results. The authors note that there is still a Y/T-ratio effect and that Y/T should be taken into account. From the comparisons involving defect-free pipe tests they infer that a similar dependence of reference stress on UTS and Y/T should exist for pipes containing corrosion defects. In particular, they say that SMYS is not an appropriate parameter on which to base the reference stress.

In pursuit of the second objective, defining the shoulder effect, the Battelle team used finite element analysis to assess the role of the shoulders between overlapping pits in controlling both Folias-type bulging and coalescence of plastically-straining pits leading to a leak or a rupture. The authors note that RSTRENG (and other currently-used corrosion assessment models) are not capable of predicting whether a failure will be a leak or a rupture. They also state that the shape factors such as the 0.67 and 0.85 used in B31G and Modified B31G, respectively, inherently involve shoulders at both ends where there are transitions to full wall thickness.

To explore the shoulder effect, a simple geometric model involving a shorter, narrower, deeper pit within a longer, wider, shallower pit was considered. Both pits were of uniform depths with the transition between pits and between full wall thickness being an abrupt step change. The Battelle team refers to this type of defect as a "nested" defect and notes that it is useful for exploring the appropriateness of the various shape factors (e.g., 0.67 for B31G, 0.85 for Modified B31G, 0.81 for PCORRC).

In their analysis of two defects (one a uniform-depth, flat-bottom defect and one a nested defect both mimicking the dimensions of those used in the Task IV experiments), the Battelle team keyed on hoop strain as the predictor of defect severity (i.e., failure pressure) and radial displacement as an indicator of bulging. Failure of a defect was defined as plastic collapse as indicated by the von Mises equivalent strain criterion. Here the report is not clear because the comparisons between model-predicted and actual failure pressures is said to be based on the Z-L criterion.

Other statements in the Task V section by the Battelle team about actual failure pressures don't agree with results quoted in their discussion of the Task IV tests. The failure pressure predicted by the analytical model using the Z-L criterion for the uniform-depth defect was 2,625 psig. By comparison the actual failure pressure of this defect stated in the discussion of the Task IV tests was 2,624 psig (stated to be 2,537 psig in the Task V discussion). The failure pressure predicted for the nested defect was 2,036 psig which is exactly the actual failure pressure of the nested defect quoted in the Battelle team's discussion of the Task IV tests. Yet, their discussion of this result under Task V implies the agreement was not so good.

In any case, the greatest value of the numerical results, according to the Battelle team, is derived from the predicted strains and displacements at various critical locations such as

bottoms of the center section across each defect and at the shoulders. These are shown in their Figure 19a and Figure 19b. Figure 19a shows trends in radial displacements at various locations within the defect as a function of normalized failure pressure (applied pressure divided by failure pressure). Figure 19b shows trends in hoop strain at various locations within the defect as a function of normalized failure pressure. The exponential-like increases in both displacements and strains are not surprising. These trends would have been expected in the actual burst tests, had the tests been equipped with strain and displacement gages. It is noted that the displacements in Figure 19a and the strains in Figure 19b continue steadily upward with normalized pressure beyond the normalized pressure level of 1.0. This indicates the importance of the criteria one uses to define failure displacement or failure strain. Such choices could certainly affect any comparisons between predicted and actual failure pressures. However, as the authors imply, the important benefit of the analyses is to indicate trends that can be used to modify existing models of corroded pipe behavior.

The authors use the trends in the two figures to suggest that shoulders in the river-bottom profile of a "naturally" created corrosion defect could have a significant effect on both the failure stress level and the mode of failure (leak versus rupture). The authors suggest that further quantifying these effects could lead to improved accuracy of Level 1 corrosion assessment models and the ability to forecast failure as a leak or a rupture if the models can be suitably modified to account for these phenomena.

Task 5 of the Battelle report delves into controversial aspects of the behavior of corroded pipe of different grades, vintages, and toughnesses. First, the report mentions the well-known fact that some older vintage materials are operated at temperatures below their fracture propagation transition temperatures. As a result if a fracture propagates in a pipeline under such conditions, extensive brittle fracture may ensue. The Battelle team, incorrectly in this reviewer's opinion, implies that corroded pipe failure under those conditions could initiate in a brittle or semi-brittle manner at levels below those predicted by one or more of the existing Level 1 corroded pipe assessment model. Aside from selective seam weld corrosion failures and failures of corrosion defects in one or two unique materials, none of the test data in the database show such outcomes. Moreover, the works of Maxey et al.[xxii], and Wilkowski et al.[xxiii] clearly show that brittle-like fracture initiation will not take place unless the material is being operated at a temperature well below its fracture propagation transition temperature. Also the work of Advantica[xxiv] on the potential for brittle behavior affecting the efficacy of corrosion prediction models suggests that: "...for the defects investigated, the *effective* (reviewer's italics) transition temperature is sufficiently low that the existing assessment methods will remain conservative."

Second, in the same section of Task 5, the authors imply that the current corrosion assessment models will underestimate the failure pressures of newer HSS materials. What few data exist for X100 materials, as shown in Figure 1 of this report, hint that the opposite may be true. The possible reasons for this behavior are not presently understood.

## Discussion of Task VI

The objectives of Task VI of Project EC2-5 were:

1. Analyze the full-scale database compiled in Tasks I and II,
2. Use the database to evaluate Level 1 severity criteria,
3. Quantify the margin of safety as a function of grade, and
4. Assess the need for further full-scale tests or numerical modeling to bridge gaps in the database and the predictive models.

The Battelle team used the database to assess the accuracy of the B31G and Modified B31G corrosion assessment models. Note that there are no real corrosion results in the database for HSS materials unless one includes the two results from the Battelle Task IV tests where "corrosion" was artificially created in an X70 material. On the basis of their Figures 20a and 20b, the authors state that B31G consolidates the data for real corrosion defects better than Modified B31G. This finding is contrary to findings of Advantica (Reference XV) which are summarized in Table 1 of this review where the opposite conclusion seems to be supported. The Battelle team's finding may be reconcilable to the findings of Reference VIII (the "continued validation of RSTRENG). In the latter study the statistics for 86 burst tests of vintage pipe materials were as follows.

Table 4 Comparisons of accuracy of models discussed in Reference VIII

| Statistic | RSTRENG | Modified B31G | B31G |
|---|---|---|---|
| 41 Ruptures | | | |
| Mean | 0.850 | 0.622 | 0.537 |
| Std. Dev. | 0.150 | 0.138 | 0.178 |
| 45 Leaks | | | |
| Mean | 0.922 | 0.675 | 0.630 |
| Std. Dev. | 0.180 | 0.221 | 0.209 |

The data in Table 4 suggest that B31G does consolidate the data better than Modified B31G for "leak" results though not for "rupture" results. The authors of the Battelle report appear to have based their finding on visual inspection of the density of data on their plots rather than on statistics of comparisons of predicted to actual failure pressures.

The Battelle authors' finding that B31G is more conservative than Modified B31G is in agreement with the findings of both the Advantica study (Reference XV) and the continued validation of RSTRENG (Reference VIII).

Why the Battelle team included test results from uniform-depth machined defects in vintage materials in their comparisons of B31G and Modified B31G in their Figures 21a and 21b is not clear. As has been pointed out in almost all studies of the data in the database including in the Battelle report, one does not expect that models such as B31G or Modified B31G with built-in shape factors less than one will accurately predict the failure pressure of a uniform-depth defect.

The authors present trends in the data in an interesting format in their Figures 21a and 21b. Figure 21a is a plot of the cumulative distributions of the ratios of strength parameters (e.g., YS/SMYS, UTS/SMTS) for the various materials involved in tests of real corrosion defects and machined defects. These plots indicate that the UTS/SMTS ratios for materials involved in tests with real corrosion defects tended to be higher than those for materials involved in tests with machined defects. Figure 21b is another plot of cumulative distributions, in this case, representing the defect lengths (normalized to $\sqrt{Rt}$), depth/thickness ratios, and ratios of predicted failure pressure to the 100%-of-SMYS pressure. Taken together these plots reflect the apparent fact that the real corrosion defects tended to fail at stress levels higher than those of machined defects even though the ranges of defect sizes were similar. It is hard to see how these trends can be separated from the effects of the predictions being made via models with shape factors less than 1. It seems that using such models to compare results of tests involving real corrosion defects with the results of tests involving machined defects would inherently give the trends portrayed in Figure 21b.

Next, the authors discuss the impact of shape factors and bulging using their Figure 22a. This figure shows the effects for the shape factors of 0.67 (B31G), 0.85 (Modified B31G), and 1.0 (RSTRENG, for example). First they acknowledge that for defects of the same overall length and depth in the same materials, those with a higher shape factor (representing defects that are shaped exactly in accord with particular shape factors), increasing failure pressures will tend to be observed for decreasing shape factors. They then use their Figure 22a to describe what one would expect, namely, that given a defect length and depth in a material of known strength, the model with the highest shape factor will give the lowest predicted failure stress.

The authors do make some useful observations in this section. One is that the empirical criteria (B31G and Modified B31G) blend the effects of shape factor and bulging obscuring the roles that these factors play in the failure of a corrosion defect. To this reviewer's knowledge, this fact has not resulted in unsafe predictions for failure pressures for real corrosion defects. The authors indirectly acknowledge this by noting that there is no reason not to use these criteria for real corrosion defects in vintage materials. However, this reviewer agrees that it is a situation that could be improved upon if further work on the behavior of corroded pipe is to occur. Secondly, they state a fact that is worth repeating: "…care always should be used in applying empirical criteria to situations that *are* (sic) outside their basis for calibration".

The authors use their Figure 22b to illustrate how much difference the shape factor makes in calculating failure pressure for shape factors of 1.0 and 0.85 and that the difference increases with increasing depth-to-thickness ratio. Their figure indicates the diameter and wall thickness of the pipe in their example, but does not mention the length of defect for which the calculations were made. It is easy to show that the difference increases with increasing defect length. None of this is unexpected. It arises from the fact that only a shape factor of 1.0 can adequately account for the severity of a uniform-depth defect. The authors may have felt that this needed saying, but the fact should be obvious to anyone who has compared test results and predictions of failure pressures for uniform-depth defects using various shape factors.

The Battelle team's discussion of grade dependence for the MoS (Margin of Safety inherent in the Level 1 assessment models) begins in the middle of Page 53 and extends to just past the

middle of Page 56 of their report. As far as this reviewer can tell, the Battelle team concludes that the Margin of Safety is not dependent on grade. This reviewer believes that the following concept is important also. What constitutes whether or not a given model is adequate for the assessment of corrosion defects is whether or not the model under consideration gives reasonable predictions of failure stress across the spectrum of pipe materials and the spectrum of corrosion anomaly configurations. A deterministic Margin of Safety for such a model can be set high enough to assure that corrosion indicated by the model to be injurious can be repaired before it becomes severe enough to cause a failure. Probabilistic margins of safety can be set as well if the distribution of predicted-to-actual failure stress for the model is well defined.

The Battelle team examined the significance of "effective" length using PCORRC to predict failure stress of the real corrosion defects in the database using both effective length and actual maximum length. Effective length as used in Battelle's report has the same definition as that used in conjunction with RSTRENG. As used in conjunction with RSTRENG, the effective length is that which gives the lowest predicted failure pressure among failure pressures calculated for all combinations of contiguous flaw depths along the "river bottom" profile of a real corrosion defect. The results of the calculations show that using effective length results in more accurate predictions of failure stress than the predictions based on actual maximum length.

In their summary of Task VI the Battelle team identified gaps in the knowledge of corrosion severity assessment criteria. The gaps are said to include the lack of adequate quantification of the effects of shape factors and bulging, the fact that the shoulder effect is not well understood, the lack of ability of current models to predict the mode of failure (leak versus rupture), and the fact the very few full-scale tests have been conducted on HSS materials. They assert that these gaps can be bridged by analysis with limited full-scale experimental verification. This reviewer agrees with the foregoing statements but takes issue with their statement that bridging the gaps is needed to avoid high visibility pipeline incidents. They presented no case of an incident having occurred because a corrosion severity assessment analysis led to an anomaly not being repaired. Most likely that is because there has been no such incident. The currently used Level 1 analyses could stand improvement, but there is no evidence that they are inadequately conservative. The more relevant circumstance is that on rare occasions, miscalls of ILI data have caused an anomaly to not be repaired leading to an incident.

## Summary of the Key Findings of Project EC2-5

Overall Battelle's report on Project EC2-5 makes several significant contributions to the understanding of corrosion defect assessment methods. These contributions include:

- Revealing that only 19 useful full-scale tests on HSS materials are included in the database of corroded pipe tests.
- Pointing out that ring test results make no meaningful contribution to the comparisons of predicted to actual failure stresses and that the ring test results should be purged from the database.
- Showing that it is possible to use ultimate tensile strength or specified ultimate tensile strength or functions thereof as the reference stress in all Level 1 assessment models in

place of an SMYS-based flow stress with no significant change in the predictive accuracy of the models.

- Presenting data that shows that reference stress is closely related to ultimate tensile strength but is also dependent on the Y/T ratio (or more precisely the strain hardening exponent) of the material.
- Showing that machined defects can be used to validate corrosion assessment models in place of real corrosion defects as long as the appropriate shape factor is applied.
- Pointing out that some Level 1 assessment models (B31G and Modified B31G in particular) may obscure the true effects and possible interactions of shape factor and bulging because of their empirical calibration.
- Presenting data that suggest a defect width effect (in addition to the well-known effects of length and depth) on failure pressure and recognizing that it should be included in any future "improved" models.
- Showing that defects can be created by accelerated corrosion and used to demonstrate a number of important factors in the behavior of corrosion defects.

The authors call for the use of sophisticated analysis methods backed by carefully designed full-scale tests if future improvements in corrosion assessment models with a focus on HSS materials are to be sought. This would seem to be a non-controversial recommendation. However, it would also seem that there are other considerations to be taken into account before anyone makes a full frontal assault on Level 1 assessment methods.

First, nowhere in the EC2-5 report is it suggested that the existing Level 1 methods are inadequate even for HSS materials. The Battelle authors state that "when ring-expansion results are culled from the database, and the shape factor is correctly quantified, both Modified B31G and B31G conservatively predict the burst test results for the HSSs…". Second, the present embodiment of B31G and particularly that of Modified B31G have been shown by the GL R6781 database of corroded pipe burst tests to be adequate certainly for the vintage materials that comprise most of the database. Third, Level 1 assessment methods are largely used to prioritize anomaly excavations based on ILI data. As such, the inaccuracies of the ILI tool descriptions of the features are likely to have much more effect on the correctness of the repair list than any of the perceived inadequacies of the Level 1 models.

Going forward, the EC2-5 report does offer a valuable guide for future analysis and experiments that will be useful if improved assessment methods for HSS materials are to be pursued.

## Summary of Findings on B31G/Mod B31G/RSTRENG

The bottom line is that the B31G/Mod B31G/RSTRENG models have been thoroughly validated for assessing the ductile failure behavior of corrosion-caused metal loss in line pipe materials up through Grade X65 in pipelines not subjected to extreme external loads. Some additional caveats are in order. The original B31G equation can give excessively conservative predictions of failure pressure for long defects. The Modified B31G equation can be applied just as easily, and does not give excessively conservative predictions of failure pressure for long actual (irregular-shaped) corrosion defects as is the case with the original B31G equation. It is noted however, that both B31G for shorter defects and Modified B31G may give un-conservative predictions for the failure pressure levels of uniform-depth defects. This is usually not a

problem when predicting failure pressure levels of actual corrosion anomalies because they are non-uniform in depth. It has been shown that the RSTRENG model gives accurate predictions for uniform-depth defects for material grades up to and including X80. However, on the basis of the defect-free burst test results examined by the Battelle team in Reference XXI where the higher-strength materials failed at levels less than predicted based on their ultimate tensile strengths, it undoubtedly will be necessary to modify the definition of flow stress when using RSTRENG or Modified B31G for failure stress predictions with X100 materials. Lastly, it is desirable to evaluate the suitability of the B31G and Modified B31G models for higher grade materials (i.e., X100 and up) by comparing predictions to burst test data on samples of these materials that contain non-uniform depth defects that simulated corrosion-cause metal loss.

## References


[i] Eiber, R.J., Maxey, W.A.., Duffy, A.R., and Atterbury, T.J., "Investigation of the Initiation and Extent of Ductile Pipe Rupture", Report No. BMI-1866, U.S. Atomic Energy Commission Contract No. w-7405-eng-92, NTIS, July 1969

[ii] Folias, E.S., "The Stresses in a Cylindrical Shell Containing an Axial Crack", Aerospace Research Laboratories, ARL 64-174, (October 1964).

[iii] Hahn, G.T., Sarrate, M., and Rosenfeld, A.R., "Criteria for Crack Extension in Cylindrical Pressure Vessels", *International Journal of Fracture Mechanics*, Vol. 5, 1969, pp. 187 – 210.

[iv] Kiefner, J.F., and Duffy, A.R., "Summary of Research to Determine the Strength of Corroded Areas in Line Pipe", presented at a Public Hearing at the U.S. Department of Transportation, July 20, 1971.

[v] *Manual for Determining the Remaining Strength of Corroded Pipelines*, A Supplement to ASME B31 Code for Pressure Piping, ASME (1984).

[vi] Kiefner, J.F., and Vieth, P.H., "A Modified Criterion for Evaluating the Remaining Strength of Corroded Pipe", American Gas Association, Catalog No. L51609 (1989).

[vii] Vieth, P. H., and Kiefner, J. F., "Database of Corroded Pipe Tests", American Gas Association (1994).

[viii] Kiefner, J. F., Vieth, P. H., and Roytman, I. "Continued Validation of RSTRENG", PRC International, Catalog No. L51749 (1996).

[ix] *Manual for Determining the Remaining Strength of Corroded Pipelines*, A Supplement to ASME B31 Code for Pressure Piping, ASME (2012).

[x] Fu, B. and Batte, A.D., 'Advanced Methods for the Assessment of Corrosion in Linepipe', UK Health and Safety Executive Summary Report, OTO 1999-051, HSE Books, 1999.

[xi] "Corroded Pipelines", Recommended Practice RP-F101, Det Norske Veritas (1999).

[xii] Stephens, D.R. and Leis, B.N., 'Development of an Alternative Criterion for Residual Strength of Corrosion Defects in Moderate to High Toughness Pipe', Proceedings of the 2000 International Pipeline Conference – Volume 2, Calgary, Alberta, Canada, American Society of Mechanical Engineers, 1-5 October, 2000.

[xiii] Ritchie, D. and Last, S., 'Burst Criteria of Corroded Pipelines – Defect Acceptance Criteria', Paper 32, Proceedings of the EPRG/PRCI 10th Biennial Joint Technical Meeting on Line Pipe Research, Cambridge, UK. 18-21 April 1995.

[xiv] "Fitness-for-Service", American Petroleum Institute Recommended Practice 579, First Edition (January 2000).

[xv] Chauhan, V., and Brister, J., "A Review of Methods for Assessing the Remaining Strength of Corroded Pipelines", GL Industrial Services, Report Number: 6781, Version 6.1 Final Report to U.S. Department of Transportation, November 2009. Reference found at: http://primis.phmsa.dot.gov/matrix/PrjHome.rdm?prj=171

[xvi] Chauhan, V., and Crossley, J., GL Industrial Services UK Ltd., Project #153H: "Corrosion Assessment Guidance for High Strength Steels" (Phase 1), Report Number R9017, to U.S. Department of Transportation, Pipeline and Hazardous Materials Safety Administration, April 2009. Reference found at: http://primis.phmsa.dot.gov/matrix/PrjHome.rdm?prj=171

[xvii] Anon: 'Guide to Methods for Assessing the Acceptability of Flaws in Metallic Structures', BS 7910:2005, Incorporating Amendment No. 1, BSi, September 2007. Reference found at: http://primis.phmsa.dot.gov/matrix/PrjHome.rdm?prj=171

[xviii] Liu, J, Mortimer, L, and Wood, A., "Project #153H Corrosion Assessment Guidance for High Strength Steels (Phase 2)", Report Number: 7930, GL Industrial Services, to: BP Exploration, US DOT PHSMA, Electicore & GL Industrial Services, November, 2009. Reference found at: http://primis.phmsa.dot.gov/matrix/PrjHome.rdm?prj=171

[xix] Liu, J., Chauhan, V., Ng, P., Wheat, S., and Hughes, C., 'Project #153J Remaining Strength of Corroded Pipe Under Secondary (Biaxial) Loading', GL Report Number R9068, Issue 2.0, June 2008. Reference found at: http://primis.phmsa.dot.gov/matrix/PrjHome.rdm?prj=171

[xx] Fu, B., Jones, C.L. and Chauhan, V., 'Guidance for Assessing the Remaining Strength of Corroded Pipeline', Pipeline Research Council International, Inc., Catalog No. L51958, Advantica Technologies, Inc., August 2002.

[xxi] Leis, B.N., and Zhu, X-K, "Assessing Corrosion Severity for High Strength Steels", Project EC2-5, Prepared for the Corrosion Technical Committee of PRCI, March 13, 2013.

[xxii] Maxey, W.A., Kiefner, J.F., and Eiber, R.J., "Brittle Fracture Arrest in Gas Pipelines", NG-18 Report No. 135, American Gas Association Catalog No. L51436, July 25, 1975.

[xxiii] Wilkowski, G., Rudland, D., Rider, D., Mincer, P., and Sloterdijk, W., "Why Old Pipelines Initiate Fracture in Ductile Manner", IPC 2006-10326, Proceedings of the IPC 2006, 2006 International Pipeline Conference, September 25-29, 2006, Calgary, Alberta, Canada.

[xxiv] Martin, M., Andrews, R.M., and Chauhan, V., "The Remaining Strength of Corroded Low Toughness Pipe", Project #153L, Advantica Report Number R9247, prepared for the U.S. Department of Transportation, Pipeline and Hazardous Materials Safety Administration, February, 2009. Reference found at :http://primis.phmsa.dot.gov/matrix/PrjHome.rdm?prj=171

**Attachment J.1**
**FINAL PROJECT SUMMARY REPORT**

## PROJECT IDENTIFICATION INFORMATION

*1. BUSINESS FIRM AND ADDRESS:* Engineering Mechanics Corporation of Columbus ($Emc^2$), 3518 Riverside Drive, Suite 202, Columbus, OH 43221.

*2. DOT SBIR PROGRAM:* Pipeline and Hazardous Material Safety Administration (PHMSA) Research Topic No: 14.2-PH1; Research Topic Title: New non-destructive evaluation methods to quantify remaining strength of line pipe steel and or pipeline fittings.

*3. DOT CONTRACT: CONTRACT NUMBER:* DTRT5715C10023

*4. PERIOD OF PERFORMANCE:* From: January 29, 2015
To: October 28, 2015

*5. PROJECT TITLE*: A Novel Approach to Establishing Remaining Strength of Line Pipe and Fittings with Corrosion Type Defects

*SUMMARY OF COMPLETED PROJECT*:

The US DOT's PHMSA is exploring technologies and methods which could increase the integrity, reliability and safety of the U.S. pipeline network. Corrosion metal loss is one of the major damage mechanisms to gas transmission pipelines worldwide. Current methods to assess the remaining strength of corroded pipelines, such as the ASME B31G (including the Modified B31G) and RSTRENG models that have been incorporated into the US Code of Federal Regulations may be inadequate and perhaps non-conservative for higher grade line pipe, X65 and above. Also recent work supported by PHMSA has shown that existing methods may be non-conservative.

During this Phase 1 effort, $Emc^2$ has established the feasibility of a novel mathematical and computational model to assess the remaining strength of pipelines and fittings with natural corrosion type defects. Specifically, (i) the "Simulation of Natural Corrosion via Computation" ($SNC^2$) methodology has been successfully demonstrated to model corrosion type defects, (ii) carefully selected laboratory experiments were conducted to demonstrate that the remaining strength of pipe and fittings is strongly determined both by the grade of the steel and for older steels the failure criterion is a function of the notch acuity at the corrosion defect, especially in higher grade (> X65 or higher) steels, (iii) the failure behavior of an older low grade steel and a modern X80 steel had ductile tearing start prior to maximum load in the blunt flaw specimens, showing that a stress-based criterion for corrosion flaws with no crack initiation criterion would over predict the failure pressure, and (iv) the methodology can be successfully scaled for commercial, rapid-time application on the cloud using high performance computational clusters. The $SNC^2$ methodology would not only be applicable to old, new, and higher grade steels, but many conditions that cannot be addressed by the B31G type methods, i.e., high longitudinal stresses, corrosion flaws that might have greater circumferential extent than axial extent, multiple corrosion patch interactions.

*The data in this final report shall not be released outside the government without permission of the contractor for a period of four years from the completion date* (October 28, 2015) *of this project from which the data was generated.*

---

*APPROVAL SIGNATURES*

| | |
|---|---|
| *PRINCIPAL INVESTIGATOR (Signature)* | *PROJECT DIRECTOR (Signature)* |
| Dr. Gery M. Wilkowski | Dr. Prabhat Krishnaswamy |
| *PRINCIPAL INVESTIGATOR (typed)* | *PROJECT DIRECTOR (Typed)* |

**Attachment J.2**
**PHASE I - COMMERCIALIZATION REPORT**

*Topic No:* Pipeline and Hazardous Material Safety Administration (PHMSA) Research Topic No: 14.2-PH1; Research Topic Title: New non-destructive evaluation methods to quantify remaining strength of line pipe steel and or pipeline fittings

*Project Title:* A Novel Approach to Establishing Remaining Strength of Line Pipe and Fittings with Corrosion Type Defects

*Firm Name:* Engineering Mechanics Corporation of Columbus ($Emc^2$),

*Address:* 3518 Riverside Drive, Suite 202

*City, State, Zip:* Columbus, OH-43221

***Provide Narrative and Relevant Statistical Data.***

*Please describe the degree of interest made by third parties, other Federal agencies, state and local governments, as well as private enterprise, in acquiring the products or services developed under this contract*

There has been significant interest from the oil and gas pipeline industry in this SBIR project ever since it was awarded. PRCI, the primary research consortium for the pipeline industry and several North American Pipeline companies joined the initial kick-off meeting at $Emc^2$'s request and have cooperated in this work by providing information and reports that are directly relevant to this topic. One pipeline company provided the corrosion data from their field for use in the sample case analyzed in the Phase I feasibility study and would like to provide both in-kind (i.e., pipe samples) and possible fund parallel efforts relative to a Phase 2 award – as the results of this work would directly benefit their operations.

*Please describe the potential market for the products or services developed under this contract for the purpose of applying it to other commercial markets.*

Upon completion of the Phase 2 project, the commercial version of the $SNC^2$ methodology will be installed on the supercomputer cloud for access remotely on the internet. The pipeline companies both in North America and worldwide will have a much more accurate and validated on-line, rapid-time, assessment tool that may be used to determine the remaining strength of fittings and pipe of all grades with any type of areal corroded defects and obtain a reliable safety margin on their operation pressure (MOP). Although we have focused on the oil/gas transmission industry, this same methodology may be of interest for processing plant piping evaluations as well as erosion-corrosion in ferritic nuclear plant evaluations

*Please describe the potential market for the products or services developed under this contract for the purpose of applying it to Government requirements.*

The $SNC^2$ methodology that will be available upon completion of the Phase 2 effort from this project will provide PHMSA regulators an independent safety assessment tool for determining the remaining strength and pressure-carrying capacity of corroded gas pipelines and fittings (and other process plant piping that might be of interest to the US Government). Based on the predictions, PHMSA can make accurate assessments for the margin of safety available for pipelines based on the corrosion profiles provided by operating pipeline companies.

*Patents & Patents Applied for have has been reported in accordance with H.14.*

No.

*Have you issued a press release or media for publicity?*

No.

*Notification of press release or other release of media for publicity has been submitted in accordance with Clause H?*

No.